

CORRELATED EXCHANGE IN THE NN INTERACTION

G. Janssen, K. Holinde, and J. Speth
 Institut für Kernphysik, Forschungszentrum Jülich GmbH,
 D-52425 Jülich, Germany

We evaluate the contribution to the nucleon-nucleon interaction due to correlated exchange in the π , ρ , and A_1/H_1 channels by means of dispersion-theoretic methods based on a realistic meson exchange model for the interaction between π and ρ mesons. These processes have substantial effects: In the pionic channel it counterbalances the suppression generated by a soft NN form factor of monopole type with a cutoff mass of about 1 GeV; in the ρ -channel it provides nearly half of the empirical repulsion, leaving little room for explicit quark-gluon effects.

21.30.+y, 13.75.Cs

I. INTRODUCTION

The study of meson-meson systems and their role in low and medium energy physics is of twofold interest. First, from a more basic viewpoint, the investigation of meson-meson interactions provides important information about the fundamental structure of strong interactions. This is especially true for the lightest system consisting of two pions. $\pi\pi$ scattering at low energies is determined by chiral symmetry and therefore plays a dominant role in chiral perturbation theory. For higher energies the study of $\pi\rho$ as well as $\rho\rho$ scattering (including the coupling to the $K\bar{K}$ channel) provides essential information on the nature of scalar resonances. Within a meson exchange (π)= $K\bar{K}$ model the $f_0(980)$ turns out to be a $K\bar{K}$ bound state and the $a_0(980)$ a $K\bar{K}$ threshold effect [1]. Second, the inclusion of meson-meson correlations is mandatory for numerous hadronic processes. In models of nucleons consisting of a quark-gluon 'core' and a meson cloud, meson-meson couplings have a large impact on the structure of nucleon form factors. In meson-exchange models of the NN interaction, which essentially include pseudoscalar and vector mesons, one has for consistency not only to include the meson-nucleon, but also the meson-meson interaction. Indeed, the correlated 2π -exchange contribution is of outstanding importance, providing the main part of the intermediate-range attraction.

In this work we want to demonstrate the important role of the contribution to the nucleon-nucleon [2] interaction provided by the exchange of a correlated pair (A corresponding letter has already been published [3]). The starting points are open questions concerning the structure of the NN vertex. Besides the coupling constant, the NN vertex function (like all baryon-baryon meson vertices) contains a form factor parametrizing the extended hadron structure and characterized, in a monopole parametrization, by a cutoff mass m_{NN} . Within the (full) Bonn potential, the best fit to the NN data requires a value of $m_{NN} = 1.3$ GeV; the resulting form factor modifies the one-pion-exchange potential for small distances ($r < 1$ fm) only. This ensures a tensor force which is strong enough to reproduce the deuteron properties, especially the D/S ratio and the quadrupole moment [4,5]. However such a hard form factor is in contradiction to information from other sources [6-9], which all favor a considerably lower value of $m_{NN} \approx 0.8$ GeV, i.e. a rather 'soft' form factor. Obviously the solution of this problem requires the inclusion of additional (short ranged) tensor contributions in the Bonn potential, which compensate for the effect of such a soft NN form factor. The exchange of a correlated pair is a natural candidate for such a contribution. Indeed, the inclusion of uncorrelated processes in the full Bonn potential already led to a reduction of the NN cutoff mass from 1.75 GeV (in the framework of a simple one-boson-exchange model (OBEP T) [2] defined likewise in time-ordered perturbation theory) to 1.3 GeV. Thus a further reduction of this value is to be expected if correlated exchange is included. This is anyway required within the strategy advocated in the full Bonn potential: namely to group and corresponding contributions together because of their counterstructure in the tensor channel. However, while the Bonn potential contains already correlated exchange (in terms of sharp mass 0 exchange), the corresponding process is not included so far.

The evaluation of correlated exchange (Fig. 1) requires the knowledge of the interaction between π and ρ mesons. We have recently derived a corresponding meson-theoretical model [10] for $\pi\rho$ scattering which provides good agreement with the existing empirical information. It is, however, not completely crossing symmetric, so that a direct evaluation of Fig. 1 (d) based on this interaction is not possible. Therefore, as in the case [11], we first evaluate the amplitude $NN \rightarrow \pi\pi \rightarrow NN$ including correlations. In a second step we use dispersion-theoretic methods to transform this amplitude into the s (NN) channel and in this way obtain the contribution of Fig. 1 (d).

A main result will be that the exchange of a correlated pair indeed generates a contribution to the NN potential

of sizable strength. In the pionic channel it leads to a tensor force component which is strong enough to cancel the effect of a soft form factor with $m_N \approx 1 \text{ GeV}$. Moreover, it provides nearly half of the empirical repulsion in the $\pi\pi$ -channel.

The structure of the paper is as follows: Sect. II provides the basic formalism, together with our model for the $\pi\pi$ amplitude; Sect. III presents and discusses the results, in the various (π, ρ, A_1, H_1) channels considered; finally, Sect. IV contains some concluding remarks.

II. FORMALISM

In the following we outline the formalism which is used to evaluate the correlated $\pi\pi$ exchange contribution to the $\pi\pi$ interaction.

A. Dispersion relation for the $\pi\pi \rightarrow \pi\pi$ amplitude

For $\pi\pi \rightarrow \pi\pi$ and $\pi\bar{\pi} \rightarrow \pi\bar{\pi}$ scattering the field theoretical scattering amplitude T is related to the standard S-matrix by

$$S_{fi} = \delta_{fi} - i(2\pi)^4 \delta^4(p_1 + p_2 - p_1' - p_2') \frac{m_N^4}{E_1^0 E_2^0 E_1 E_2} T_{fi} \quad (1)$$

If we neglect isospin for the moment, the s-channel ($\pi\pi \rightarrow \pi\pi$) amplitude can be written as

$$T_s(p_1^0; p_2^0; p_1; p_2) = \bar{u}(p_1^0; \lambda_1) \bar{u}(p_2^0; \lambda_2) \hat{T} u(p_1; \lambda_1) u(p_2; \lambda_2) \quad (2)$$

where

$$u(p; \lambda) = \frac{1}{2m_N} \frac{E(p) + m_N}{2E(p) + m_N} \chi_{\lambda} \quad (3)$$

is a Dirac helicity spinor normalized to $\bar{u}u = 1$. (The spin dependence is suppressed on the left hand side of Eq. (2).) For on-shell scattering, \hat{T} can be expressed as a linear combination of five invariant operators \hat{C}_j ; the expansion coefficients c_j are scalar functions of the Mandelstam variables $s = (p_1 + p_2)^2$ and $t = (p_1 - p_1')^2$. (u is not independent, but given by $u = 4m_N^2 \chi_{\lambda} \delta_{\lambda\lambda'}$.) \hat{T} can then be written as

$$\hat{T} = \sum_{j=1}^5 c_j(t; s) \hat{C}_j \quad (4)$$

In contrast to our former work dealing with correlated $\pi\pi$ exchange [11] we now use, instead of the so-called perturbative invariants (see Ref. [11]) the Fermi-invariants

$$\begin{aligned} S &= (I)^{(1)} (I)^{(2)} \\ P &= (S)^{(1)} (S)^{(2)} \\ V &= (V)^{(1)} (V)^{(2)} \\ A &= (A)^{(1)} (A)^{(2)} \\ T &= (T)^{(1)} (T)^{(2)} \end{aligned} \quad (5)$$

where $\chi_{\lambda} = \frac{1}{2} [\chi_{\lambda}^{(1)} ; \chi_{\lambda}^{(2)}]$.

Correspondingly, the amplitude for the t-channel ($\pi\bar{\pi} \rightarrow \pi\bar{\pi}$) process defined in Fig. 2 then reads

$$T_t(p_1^0; p_2^0; p_1; p_2) = \bar{v}(p_1^0; \lambda_1) \bar{v}(p_2^0; \lambda_2) \hat{T}_t v(p_1; \lambda_1) v(p_2; \lambda_2) \quad (6)$$

Here

$$v(p; s) = \frac{s}{2m_N} \frac{E(p) + m_N}{2} j > \quad (7)$$

is the Dirac spinor for an antiparticle. Due to crossing symmetry \hat{T} can be represented in the same way as before (Eq. (4)), with precisely the same functions c_j , however in a different s, t domain obtained by replacing p_1^0 by p_1^0 and p_2 by p_2 .

The functions c_j arising from (correlated) exchange are assumed to fulfill a dispersion relation over the unitarity cut,

$$c_j(t; s) = \frac{1}{(m + m)^2} \int_{t^0}^Z \frac{\text{Im } c_j(t'; s) dt'}{t' - t} \quad (8)$$

(Throughout we take the to be a stable particle with $m = 769 \text{ MeV}$.) Thus the c_j can be determined if their imaginary part is known in the pseudophysical region ($t^0 = (m + m)^2$) of the t -channel reaction and for $s = 4m_N^2$.

B. Determination of the spectral functions from unitarity

The required information about the spectral functions $c_j(t^0; s) = \text{Im } c_j(t^0; s)$ can be obtained from the relevant unitarity relation (cf. Fig. 3)

$$i \langle N \bar{N} | \hat{T}^X | \hat{T}^Y | N \bar{N} \rangle = \sum \langle N \bar{N} | j^Y | j \rangle \langle j | N \bar{N} \rangle \quad (4) \quad (k_1 + k_2 + p_1^0 = p_1) \quad (9)$$

where is a phase-space factor. We first do a partial wave decomposition,

$$\begin{aligned} T_t(p^0_N, p^0_N; p_N, p_N; t) &= \frac{1}{4} \sum_J (2J+1) d^J_0(\cos \#) T_t^J(p^0_N, p^0_N; p_N, p_N; t) \\ t(k; p_N, p_N; t) &= \frac{1}{4} \sum_J (2J+1) d^J(\cos \#) t^J(k; p_N, p_N; t) \end{aligned} \quad (10)$$

with

$$p^0_N, p^0_N; p_N, p_N; t = ; N, N; \quad (11)$$

p, p^0, k being the relative 3-momenta in the center-of-mass (cm) system and the angles $\# = \angle(p; p^0)$, $\# = \angle(p; k)$. After transformation into LSJ basis Eq. (9) goes into

$$\begin{aligned} \text{Im} [T_t^J(p_0; L^0 S^0; p_0; L S; t)] \\ = C \sum_L [t^J(k_0; L-1; p_0; L^0 S^0; t)]^p t^J(k_0; L-1; p_0; L S; t) \quad J_N(L^0 S^0; L S) \end{aligned} \quad (12)$$

where $C = (32)^{2p} t$ and p_0, k_0 denote the on-shell momenta of the $N \bar{N}$ and system, respectively.

As for the 2^- -exchange case, we want to restrict ourselves to the $J = 0; 1$ exchange contributions, which act in channels corresponding to the quantum numbers of the pion ($J = 0$), and the ρ, A_1 , and H_1 meson ($J = 1$). Table I shows the quantum numbers and possible transitions from the $N \bar{N}$ to the system obtained from the conditions

$$(-1)^{L_N \bar{N} + 1} = P P (-1)^L = (-1)^L \quad (13)$$

$$(-1)^{L_N \bar{N} + S_N \bar{N} + I} = G G = 1 \quad (14)$$

due to parity and G-parity conservation. We therefore obtain for the different relevant channels

$$\begin{aligned} {}^0N(00;00) &= C (t_{0+}^0)^y t_{0+}^0 \\ {}^1N(01;01) &= C (t_{1+}^1)^y t_{1+}^1 \\ {}^1N(21;01) &= C (t_{1+}^1)^y t_{1+}^1 \\ {}^1N(01;21) &= C (t_{1+}^1)^y t_{1+}^1 \\ {}^1N(21;21) &= C (t_{1+}^1)^y t_{1+}^1 \\ {}^1N(11;11) &= C [(t_{1+}^1)^y t_{1+}^1 + (t_{1+}^1)^y t_{1+}^1] A_1 \\ {}^1N(10;10) &= C [(t_{0+}^1)^y t_{0+}^1 + (t_{0+}^1)^y t_{0+}^1] H_1 \end{aligned} \quad (15)$$

The knowledge of \mathcal{J}_N determines the spectral functions. With the help of Appendix A, we have explicitly

$$\begin{aligned}
 P(s;t) &= \frac{1}{8} \cos^2 \theta \, {}^0N(00;00) \\
 f_{S;V;T;A;g}(s;t) &= 0 \\
 S(s;t) &= \frac{1}{16} \cos^2 \theta \left[\frac{1}{2} (1)^2 {}^1N(01;21) + (2^2 + 5 + 2) {}^1N(21;21) - 2(1)^2 {}^1N(01;01) \right] \\
 V(s;t) &= \frac{1}{16} \cos^2 \theta \left[\frac{1}{2} (2 + 1) {}^1N(01;21) + (2^2 + 2) {}^1N(21;21) + 2(1) {}^1N(01;01) \right] \\
 T(s;t) &= \frac{1}{128} \cos^2 \theta \frac{1}{m_N^2} \left[\frac{1}{2} (2 + 2) {}^1N(01;21) + (2 + 1) {}^1N(21;21) - 2(1) {}^1N(01;01) \right] \\
 P_A(s;t) &= \frac{1}{16} \cos^2 \theta \left[\frac{1}{2} (2 + 2) {}^1N(01;21) + (2 + 1) {}^1N(21;21) - 2(1) {}^1N(01;01) \right] \\
 A(s;t) &= 0 \\
 P^{A_1}(s;t) &= \frac{3}{16} \cos^2 \theta \, {}^1N(11;11) \\
 A^{A_1}(s;t) &= \frac{3}{16} \cos^2 \theta \, {}^1N(11;11) \\
 f_{S;V;T;g}^{A_1}(s;t) &= 0 \\
 P^H(s;t) &= \frac{3}{8} \cos^2 \theta \, {}^1N(10;10) \\
 f_{S;V;T;A;g}^H(s;t) &= 0
 \end{aligned} \tag{16}$$

with $E^2(p) = m_N^2$ and $\cos^2 \theta = 1$.

C. Microscopic model for the $N\bar{N}$ process

The determination of the spectral functions ρ_i requires the knowledge of the transition amplitude $t_{N\bar{N}}$ including correlations. In our dynamical model whose structure is visualized in Fig. 4 this quantity is obtained from

$$t_{N\bar{N}} = v_{N\bar{N}} + v_{N\bar{N}} G T ; \tag{17}$$

where $v_{N\bar{N}}$ is the transition potential specified later, G is chosen to be the Blankenbecler-Sugar [12] propagator of the system, and T is the transition amplitude essentially taken from the dynamical model [10]. After partial wave decomposition Eq. (17) reads more explicitly, in the helicity state basis,

$$\begin{aligned}
 t^J(k; p_N \bar{N}; t) &= v^J(k; p_N \bar{N}; t) \\
 + \int_0^X \int_0^Z \frac{d^3k}{(2\pi)^3} \frac{v^J(k^0; p_N \bar{N}; t) T^J(k; k^0; t)}{(k^0)^2 (k^0)^2} & ;
 \end{aligned} \tag{18}$$

1. The transition potential $v_{N\bar{N}}$

Our model for the transition potential $v_{N\bar{N}}$ is based on nucleon and exchange, together with an ω pole term (Fig. 5). In principle, further pole terms exist in the channels considered in this work which are, however, not included

in the present calculations for the following reasons: In case of the pion, its mass lies far below the threshold so that such a diagram has a negligible influence on the dispersion integral, Eq. (8). In case of the A_1 and H_1 little is known about their coupling strength to the nucleon. On the other hand, the (bare) $!NN$ coupling constant can be fixed by adjusting the final result to the empirical NN repulsion (see below).

The starting point for the evaluation of the corresponding potential expressions is the set of interaction Lagrangians

$$\begin{aligned}
 L_{NN} &= \frac{f_{NN}}{m} \bar{\psi} \gamma_5 \psi \phi \sim \text{etc.} \\
 L_{NN} &= g_{NN} \bar{\psi} \psi + \frac{1}{4m_N} \bar{\psi} (\not{\partial} \psi - \psi \not{\partial}) \\
 L_N &= \frac{f_N}{m} \bar{\psi} \gamma_5 \psi \phi + \text{h.c.} \\
 L_N &= \frac{f_N}{m} \bar{\psi} \gamma_5 \psi \phi + \text{h.c.} \\
 L_{!NN} &= g_{!NN} \bar{\psi} \psi \phi \\
 L_{!} &= g_{!} \bar{\psi} \psi \phi \sim \text{etc.}
 \end{aligned} \tag{19}$$

We then obtain for the structure of the potential matrix elements
nucleon exchange:

$$v_s = i f F^2 \frac{f_N g_N}{m} \frac{v(q_2) \gamma_5 \gamma_2 [\not{p}_x + m_N]}{p_x^2 m_N^2} = \frac{1}{4m_N} \not{k}_1 + \frac{1}{4m_N} \not{k}_1 u(q_1) \tag{20}$$

exchange:

$$\begin{aligned}
 v_s &= i f F^2 \frac{f_N g_N}{m m} v(q_2) (k_2) S \gamma_5 [(k_1) (k_1)] u(q_1) \\
 S &= \frac{\not{p}_x + m}{p_x^2 m^2} g + \frac{1}{3} + \frac{2}{3m^2} p_x p_x \frac{1}{3m} (p_x p_x - p_x p_x)
 \end{aligned} \tag{21}$$

! exchange:

$$v_t = f F^2 \frac{g_{!}^{(0)} g_{!}^{(0)}}{m_{!}} \frac{\not{p}_t}{p_x^2 (m_{!}^{(0)})^2} \gamma_0 (k_1) v(q_2) u(q_1) \tag{22}$$

where k_1 (k_2) and q_1 (q_2) denote the four-momenta of the () and nucleon (antinucleon), respectively. p_x is the momentum of the exchanged particle; for the ! exchange term, in the cm system, $p_x = (\vec{t}; 0)$. γ_0 is the polarization vector for the outgoing meson. F^2 denotes the product of vertex form factors, for which we used

$$\begin{aligned}
 \text{s channel: } F^2 &= \frac{2^2 M_X^2}{2^2 p_x^2} \frac{2^2 M_X^2}{2^2 p_x^2} \\
 \text{t channel: } F^2 &= \frac{2^2 p_x^2 + m_X^2}{2^2 p_x^2 + [!(k) + !(k)]^2} \frac{2^2 M_X^2 + m_X^2}{2^2 M_X^2 + 4E(p_x)^2};
 \end{aligned} \tag{23}$$

where X stands for the exchanged particle. f denotes the isospin factor; corresponding values are given in Table II. The coupling constants are either experimentally known or fixed from our former studies. An exception is the bare !NN coupling $g_{!}^{(0)}$ which, as mentioned before, will be fixed later. Values for coupling constants and cutoff masses used are given in Table III. [The s-channel cutoff masses have been adjusted to reproduce the overall strength of

$\overline{N N}$! potential used in earlier studies [13]. This potential produces good agreement with empirical information above the $\overline{N N}$ threshold, but is based on a different ρ -shell behavior (time-ordered perturbation theory rather than BbS).] The zero-th components of momenta are determined by the BbS reduction [14] to be $q_1^0 = q_2^0 = \frac{1}{2} \sqrt{t-2}$, $k_1^0 = \frac{1}{2} \sqrt{t+1} - (k) - (k)$, and $k_2^0 = \frac{1}{2} \sqrt{t+1} - (k) - (k)$. The potential matrix elements are then decomposed into LSJ partial waves in the standard way. Further u-channel diagrams arising from N and ρ exchange can be taken into account by adding a factor of 2 in the (partial wave) s-channel contributions.

2. The amplitude T_{ρ}

Our model for the correlation amplitude T_{ρ} [10] is generated from the three-dimensional BbS [12] scattering equation

$$T(k^0; k; E) = V(k^0; k; E) + \int d^3 k^0 V(k^0; k^0; E) G(k^0; E) T(k^0; k; E); \quad (24)$$

(k, k^0, k^0 are corresponding on relative momenta) with the potential V containing the diagrams shown in Fig. 6. It contains, besides non-pole pieces, pole terms with bare parameters (masses, coupling constants) which are renormalized by the iteration in Eq. (24) and in this way acquire their physical properties. Basic interaction Lagrangians have been taken from the nonlinear ρ -model in the meson sector where the vector mesons are introduced as gauge bosons of a hidden SU(2) or SU(3) symmetry. In this way one obtains the coupling of the ρ to the meson and to itself, i.e. $L_{\rho\pi\pi}$ and $L_{\rho\rho\rho}$, with a unified value for the coupling constants. Note that we have left out a corresponding pion pole term. The reason is the very small pion mass lying far below the ρ threshold, so that such a diagram should have a negligible influence in the dispersion integral, Eq. (8).

In addition to the model presented in Ref. [10] the present calculations include the H_1 ($J^P = 1^+, I^G = 0^-$) channel; therefore V now contains an H_1 -pole term. The corresponding expression is analogous to the A_1 -term, see [10], with the isospin factor $f = 3 I_{\rho,0}$, bare coupling constant $(g_{H_1}^{(0)})^2 = 4 = 1.3$ and bare mass $m_{H_1}^{(0)} = 1100$ MeV. As Fig. 7 shows, we obtain a reasonable description of the H_1 mass distribution, although compared to the A_1 case the model underestimates the empirical situation somewhat. Still, the rough agreement should be sufficient to estimate the relevance of the H_1 channel for the correlated ρ exchange $\overline{N N}$ interaction.

D. $\overline{N N}$ interaction arising from correlated ρ exchange

In the last section we specified the dynamical model for the $\overline{N N}$! amplitude, which yields the spectral functions $(s; t)$, Eq. (17). The dispersion integral, Eq. (8), then determines the invariant amplitudes $c_j(t; s; t < 0)$ and thus the scattering operator \hat{T} (Eq. (4)). The various $\overline{N N}$ potential contributions are then obtained by sandwiching \hat{T} between in- and outgoing spinors (cf. Eq. (2)).

Such a calculation can be directly pursued for the ρ and A_1 channel since these spectral functions do not depend on $\cos\theta$, which is, in terms of the Mandelstam variables,

$$\cos\theta = \frac{4m_N^2 - t - 2s}{t - 4m_N^2} = \frac{u - s}{t - 4m_N^2}; \quad (25)$$

When transforming into the $\overline{N N}$ channel, corresponding values for $s > 4m_N^2$ have to be inserted, and, in principle, the t -dependence in $\cos\theta$ should be integrated over in the dispersion integral. However, it is then not guaranteed that the typical structure of s-channel vector meson exchange is obtained. Namely, starting from the conventional vector meson Lagrangian,

$$L = g \bar{\psi} \gamma_\mu V^\mu \psi + f \partial_\mu \psi \partial^\mu V^\nu \psi \quad (\partial V \cdot \partial V); \quad (26)$$

one obtains for the scattering operator (m_V is the mass of the vector meson)

$$\hat{T} = \frac{1}{t - m_V^2} g^2 [V] - gf [V + \frac{u - s}{4m_N^2} S + \frac{t}{8m_N^2} T + \frac{u - s}{4m_N^2} P] - f^2 [\frac{t}{8m_N^2} T + \frac{u - s}{4m_N^2} P]; \quad (27)$$

Obviously a characteristic factor $u - s - \cos\theta$ occurs in front of the invariants S and P as well as a factor t in front of T . This structure is, for the case of ρ exchange, of decisive importance for a correct behavior of the $\overline{N N}$

interaction. However, since we have to apply approximations when evaluating the dispersion integral (by introducing a cutoff $t_c = 4m_N^2$), this structure is not automatically obtained when doing a straightforward calculation. Therefore we decided to transform these factors directly into the NN channel and to apply the dispersion integral for the remaining part of the spectral functions. (In a more formal language, new invariant operators have to be defined which include these factors.) Trivially the results are then forced to have the structure of s -channel vector meson exchange.

Another important modification of the above formulas remains to be introduced. So far, by construction (see Fig. 4), our results contain not only the correlated part we are interested in, but also the uncorrelated contribution, cf. Fig. 1. Therefore the latter has to be removed. We do this by subtracting the Born term part of the $^J NN$ functions of Eq. (15), which leads to new functions $^J N_{\text{corr}}$ given by

$$^J N_{\text{corr}}(00;00) = C [(t_{0+}^0)^{y_{t_{0+}^0}} (v_{0+}^0)^{y_{v_{0+}^0}}] \quad (28)$$

for the pion and analogous extensions for the other channels. These new functions $^J N_{\text{corr}}$ are actually used when evaluating the spectral functions by means of Eq. (17).

We still have to transform the isospin part of the $N\bar{N} \rightarrow N\bar{N}$ amplitude into the s -channel. Resulting isospin factors are provided by the isospin crossing matrix [15]. In general we have

$$\begin{aligned} f_{NN}^{I=0} &= \frac{1}{2} (f_{NN}^{I=0} - 3f_{NN}^{I=1}) \\ f_{NN}^{I=1} &= \frac{1}{2} (f_{NN}^{I=0} + f_{NN}^{I=1}) \end{aligned} \quad (29)$$

for the connection of isospin factors in both channels. The factors for our $N\bar{N} \rightarrow N\bar{N}$ amplitude are already implicitly taken into account by including corresponding factors in $v_{N\bar{N}}^I$ and T_{ij} . For the (isospin zero) H_1 channels we thus have $f_{NN}^{I=0} = \delta_{I,0}$ whereas in A_1 and A_2 we have $f_{NN}^{I=1} = \delta_{I,1}$. Therefore our final result for the correlated exchange NN potential can be written as operator in isospin space in the following way:

$$V_{\text{corr}} = \frac{1}{2} \sum_{i=H_1} \sum_{j=A_1} \int_{t_0}^{t_c} dt \frac{t_0 - t}{t_0 t} C_{ij} + \dots \quad (30)$$

where C_{ij} , according to the foregoing discussion, are matrix elements between nucleon helicity spinors of slightly modified invariants $(u-s)S, (u-s)P, V, A, tT$. The factor $\frac{1}{(2^3)^3} \frac{m_N^2}{E_1 E_1^0 E_2 E_2^0}$ arises because V_{corr} is to be defined as part of the Bonn potential whose T -matrix is defined by

$$S_{fi} = f_{ij} \int d^4(p_1 + p_2) T_{fi} \quad (31)$$

In order to be used in a scattering equation the resulting potential must be given on shell, as function of the in- and outgoing cm relative momenta and total energy in the s (NN) channel, i.e. $V = V(p^0; p; E_{\text{cm}})$. On shell, for $p^0 = p = p_0$ with $E_{\text{cm}}^2 = 4(m_N^2 + p_0^2)$, the relation of these variables to the Mandelstam variables is unique and given by

$$\begin{aligned} s &= 4E(p)^2 \\ t &= 2p^2(1 - \cos\theta) \\ u &= 2p^2(1 + \cos\theta) \end{aligned} \quad (32)$$

Half on-shell, i.e. for $p^0 \neq p$, we take the plausible prescription $t = (p - p^0)^2$ and $s = 4E(p)E(p^0)$, which of course agrees with Eq. (32) on shell. Dependence on the starting energy is assumed to be of the same type as in time-ordered perturbation theory applied in the Bonn potential. Here the propagator of an exchanged meson reads

$$\frac{1}{(E_{\text{cm}} - E(p) - E(p^0) - i\epsilon)} \quad (33)$$

In order to obtain a natural generalization of this expression we first define the on-shell energy of an exchanged system', $t_0 + (p - p^0)^2 = \frac{t_0}{t}$ and replace the energy denominator of the dispersion integral by the on-shell-equivalent expression

$$\frac{1}{t_0 - t} \rightarrow \frac{1}{(E_{\text{cm}} - E(p) - E(p^0) - i\epsilon)} \quad (34)$$

Finally the resulting potentials have to fall off sufficiently rapidly in order to be able to solve the scattering equation. For this reason we introduce an additional form factor, $\frac{n^2 m^2}{n^2 t} \rightarrow \frac{n^2 t_0}{n^2 t}$, with $n = 5$ GeV, $n = 5$, into the dispersion integral. The large cutoff mass chosen ensures that the results are not modified on shell.

It is convenient to parametrize our correlated exchange results in terms of single, sharp-mass effective meson exchange, as done for the analogous case of correlated in the NN [11] and N [16] system. For reasons to be discussed below, this can only be done successfully for the π and ρ channel contributions. For an effective π^0 the scattering operator reads

$$\hat{T} = g_{\pi NN}^2 \frac{1}{t - m_{\pi^0}^2} P \quad (35)$$

For the ρ^0 , the expression has already been given in Eq. (27). By comparison of the coefficients belonging to the invariants with the corresponding dispersion-theoretic terms one can determine an effective coupling constant, which will in general be t -dependent. For example we have for the pionic channel

$$g_{\pi NN}^2(t) \frac{1}{t - m_{\pi^0}^2} = \frac{1}{2} \frac{6}{4} \frac{1}{(m_{\pi^0} + m_N)^2} \int_{t_0}^Z \frac{P(t')}{t' - t} dt' \quad (36)$$

The effective mass m_{π^0} is chosen such that $g_{\pi NN}$ becomes essentially independent of t . It turns out that for the H_1 channel such a mass cannot be found. For channels involving several invariants, different coupling constants (and masses) are obtained which depend on the specific invariant for which the comparison is made. Obviously such a parametrization is successful if the resulting values only weakly (if at all) depend on the invariant chosen. This is the case for the π -channel but not for the A_1 -channel.

III. RESULTS AND DISCUSSION

Having introduced the necessary formalism for the evaluation of correlated exchange we now present the results and investigate their consequences for the NN interaction. We start with the results obtained in the t -channel, i.e. for the $N\bar{N} \rightarrow N\bar{N}$ amplitude and the spectral functions. We then discuss the properties of the resulting potential contribution, which is obtained from the (dispersion-theoretic) transformation into the s -channel, and point out its role within the Bonn meson exchange NN interaction [2].

A. The π channel

The pionic channel of correlated exchange is of special importance. As mentioned in the introduction it is a natural candidate to provide additional (short ranged) tensor force required to fit empirical NN data with models using a realistic, soft NN form factor.

Fig. 8 shows the $N\bar{N} \rightarrow N\bar{N}$ (on-shell) potential $v_{N\bar{N}}(t)$ and the corresponding amplitude $t_{N\bar{N}}(t)$ obtained from Eq. (17), which contains the effect of correlations. The purely imaginary potential has a strong increase at the pseudophysical threshold and a maximum near $t = 50m_{\pi^0}^2$. Correlations strengthen this maximum; in addition they generate a real part in the amplitude. Note that these modifications act quadratically in the $N\bar{N} \rightarrow N\bar{N}$ amplitude and therefore also in the NN potential, so that the net effect of correlations is stronger than Fig. 8 suggests.

Indeed, the spectral function $\rho_P(t)$ in Fig. 9 demonstrates that the piece due to correlated exchange has a considerable strength, although it is smaller than the uncorrelated part generated by the transition potential only. One has to keep in mind that a good part of the latter contribution consists of iterative box diagrams involving NN intermediate states, which are not part of V_{NN} but are generated by the NN scattering equation. Consequently the role of uncorrelated processes in V_{NN} is considerably smaller than suggested from the figure.

The spectral function of the correlated part has a clear maximum at about $t = 60m_{\pi^0}^2$, thus representing the mass distribution of a broad, heavy effective particle with pionic quantum numbers. A rough parametrization of this contribution by sharp-mass particle exchange appears to require a mass of about 1 GeV, noticeably smaller than chosen in Ref. [17] for the phenomenological π^0 .

In the s -channel we first demonstrate the influence of the resulting on-shell potentials in the 3S_1 , 3D_1 and 1S_0 partial waves as function of the nucleon lab energy. In Fig. 10 the dotted and dashed curves show the corresponding one-pion-exchange (OPE) potentials; obviously there is a strong suppression of OPEP when the NN cutoff mass

is reduced from the value of 1.3 GeV used in the full Bonn potential to 1 GeV. Most importantly, the addition of the potential due to correlated exchange in the pionic channel to the dotted curve restores the original tensor force strength; obviously it is able to counterbalance the suppression induced by the smaller NN cutoff mass. The 3S_1 – 3D_1 partial wave is of special importance in this connection since it exclusively contains a tensor force component, which is decisive for a realistic description of deuteron properties.

It should be added that the above result is in remarkable agreement with a previous calculation of the NN form factor [3], Fig. 11, which consistently used the same t-matrix and NN! transition potential, and independently arrived at $m_{NN} = 1 \text{ GeV}$.

As discussed in Sect. III E, correlated exchange in the π and ρ channels can be parametrized by sharp-mass one-boson-exchange (OBE) potentials, provided that the effective coupling constants are allowed to become t-dependent. Fig. 12 shows such coupling constants for the exchange of a heavy ρ for various chosen masses of ρ . Obviously the coupling becomes t-independent for a mass of 1020 MeV, quite near the maximum of the correlated spectral function in Fig. 9, and the resulting coupling constant is $g_{\rho NN}^2 = 4.9$. If we choose $m_\rho = 1200 \text{ MeV}$ as in [17], the resulting coupling constant is noticeably t-dependent; its strength is much smaller than used in [17]. There are two reasons for this discrepancy: First the authors of [17] applied a 0NN form factor, which reduces the strength at $t=0$ (relevant for NN scattering) by more than a factor of 2. Second, the strength of the ρ was phenomenologically chosen in [17] to compensate for a much softer NN form factor, with a cutoff mass of 800 MeV. (Indeed a much smaller value ($g_{\rho NN}^2 = 4.70$) is sufficient to compensate for a form factor with $m_{NN} = 900 \text{ MeV}$ [18].) Obviously correlated exchange can only partly explain the phenomenological ρ ; another possible mechanism is correlated exchange [19] (where π stands for correlated exchange in the S-wave channel).

In order to show that the compensation for a softer NN form factor by correlated exchange is valid not only for on-shell potentials, but also for NN amplitudes and observables, we extrapolate the correlated exchange off-shell as described in Sect. IID, add this piece to the (full) Bonn potential (with a reduced NN cutoff mass of 1 GeV) and solve the relativistic Schrödinger equation relevant for the Bonn potential. Only a slight readjustment of the coupling of the isospin-one scalar meson (σ in [2]) in the original Bonn potential is required in order to obtain again a good description of NN phase shifts.

As Table IV demonstrates convincingly the deuteron observables also can be reproduced with a considerably softer NN form factor (characterized by $m_{NN} = 1 \text{ GeV}$), provided that correlated exchange in the pionic channel is included.

B. The ρ -channel

Since the mass of the physical ρ -meson is only slightly below the threshold, genuine pole terms have been included in the amplitude [10] as well as in our model for the transition potential $v_{NN!}$. As Fig. 13 (a) shows, the contribution of such pole terms leads to a reduction of the (imaginary) transition potential above the threshold, whose amount depends on the value of the bare coupling constant $g_{\rho NN}^{(0)}$. (The reason for our choice $g_{\rho NN}^{(0)} = 4.40$ will be discussed later.) Fig. 13 (b) shows the resulting amplitude $t_{NN!}$. Similarly to the pionic channel, correlations enhance the maximum of the amplitude near threshold.

The inclusion of the ρ -meson pole terms in our dynamical model ensures that the imaginary part of the $NN! \rightarrow NN$ amplitude, and therefore the resulting NN potential, contains, besides 'true' correlated exchange (Fig. 14 (e)) generated by the non-pole parts of the corresponding amplitudes, also genuine ρ exchange processes (Fig. 14 (a)–(d)). Corresponding propagators and vertex functions are dressed by loop corrections. For example, the ρ propagator has the following structure (for details we refer the reader to [10]):

$$d = \frac{1}{t - (m_\rho^{(0)})^2} + \int_0^1 dt' \frac{f^{(0)}(t') G(t, t') f(t)}{(t - (m_\rho^{(0)})^2)^2} ; \quad \text{with} \quad (t) = f^{(0)} G f ; \quad (37)$$

where $f^{(0)}$ and f are bare and dressed $\rho\rho$ vertex functions, respectively, and G denotes the ρ propagator.

The bare parameters $g_{\rho NN}^{(0)}$ and $m_\rho^{(0)}$ have been adjusted such that d has a pole at $t = m_\rho^2$. The imaginary part of the $NN! \rightarrow NN$ amplitude, and therefore the corresponding spectral functions, consist of a δ -function at $t = m_\rho^2$, which precisely corresponds to the exchange of a (physical) ρ -meson with point-like ρNN coupling, i.e. without any form factor. However it is important to realize that d , and therefore the diagrams in Fig. 14 (a)–(d), provide a further contribution, since intermediate states make the self-energy complex above the threshold. Such intermediate states likewise occur at the vertices in diagrams (b)–(d), leading to additional contributions to the spectral functions.

Fig. 15 shows the resulting spectral functions. Note that although we assumed the bare ρNN coupling to be of pure vector type, small contributions to S , T , and P occur, which are generated by the loops in Fig. 14 (b)–(d). First

we have the π -function piece (dashed); above π threshold we have additional contributions from diagrams 14 (a)-(d) (dash-dotted) which have opposite sign to the π -function. They act as vertex corrections which suppress the point-like coupling of π exchange and thus generate a form factor effect. Finally there is a sizable non-pole contribution (dotted curve); throughout it has opposite sign to the part generated by the vertex corrections and roughly counterbalances their effect, a fact found already in the pionic channel.

Again, after presenting the results in the t-channel, we now want to look at the corresponding on-shell potentials in the s-channel. Since we deal with rather short-ranged contributions we show, as two characteristic examples, the results for the 1S_0 and 3P_1 partial waves (Fig. 16). Note that the bare πNN coupling ($g_{\pi NN}^{(0)} = 4.40$), which determines the size of diagrams (a)-(c), has been chosen such that the total repulsion generated by all diagrams of Fig. 14 agrees (at low energies) with the effective π exchange in the Bonn potential needed empirically. The dashed curves are generated by the π -functions in Fig. 15, with a predicted renormalized coupling constant of $g_{\pi NN}^2 = 11.0$. Apparently this contribution alone provides almost the same repulsion as in the Bonn potential although the coupling constant is about a factor of 2 smaller. The reason is that the phenomenological form factor in the Bonn potential, with the monopole cutoff mass (1.5 GeV) of only twice the π mass, leads to a strong reduction of the coupling constant in the physical region ($g_{\pi NN}^2(t=0) = 10.6$). The vertex corrections (generated by diagrams (a)-(d) above π threshold) strongly reduce the repulsion in the physical region, leading to the dash-dotted curve. This suppression is essentially cancelled by the 'true' correlated π exchange (diagram 14 (e)), as already demonstrated for the spectral functions. Obviously the latter contribution is remarkably strong; it explains about 40% of effective π exchange.

The new reduced coupling constant (11.0) is still about a factor of 2 larger than provided by customary SU(3) estimates, which use $g_{\pi NN}^2 = 9g_{\pi NN}^2$. Thus with $g_{\pi NN}^2 = 4 = 0.55$ as determined by Hoehler and Pietarinen [20] we have $g_{\pi NN}^2 = 4 \cdot 5$. Note however that the above relation between π and ρ coupling constants is based, apart from ideal mixing, on the assumption of vanishing πNN coupling. For $g_{\pi NN}$ unequal to zero the above relation goes into

$$g_{\pi NN} = 3g_{\rho NN} \frac{P - 2g_{\rho NN}}{2g_{\rho NN}} \quad (38)$$

Thus if we take $g_{\rho NN} = -g_{\pi NN}$ (which amounts to a rather small deviation from zero) we have $g_{\pi NN}^2 \approx 20g_{\rho NN}^2$, in rough agreement with our results. Such a value for the ρNN coupling to the nucleon and the negative sign is well conceivable, if the ρ couples to the nucleon via the $K\bar{K}$ continuum [21].

As discussed before, for practical reasons it is convenient to parameterize also the non-pole contribution of diagram 14 (e) by an effective one-boson-exchange. Results are shown in Fig. 17, for the dominant vector as well as the tensor coupling. Obviously they can be reasonably represented by $g_{\rho NN}^2 = 4 = 8.5$, $f_{\rho NN} = g_{\rho NN} = 0.4$, and $m_{\rho} = 1120$ MeV. Using the mass of the physical ρ meson $m_{\rho} = 782$ MeV we find a (t-dependent) effective ρ coupling strength characterized by $g_{\rho NN}^2 \approx 4$. It is interesting to note that the suppression of the tensor coupling, in some sense enforced in the pole terms by assuming the corresponding bare coupling to be zero, also happens in the non-pole term.

C. The A_1/H_1 -channel

After the discussion of the π and ρ channel we now want to investigate the A_1 and H_1 channels together since their structure is very similar. Compared to the π and ρ channels we have important differences. First the A_1 as well as the H_1 mass lie above the π threshold, and both particles decay with a very large width into π . Consequently their propagators now acquire a pole in the complex plane. Second, in contrast to the π and ρ channels, the Bonn potential [2] does not contain A_1/H_1 OBE contributions, which could be used to fix the bare $A_1 NN$ and $H_1 NN$ coupling constants, as was done in the π channel. Since there is no other a priori information about these couplings, we will in this first extrapolatory study, simply put them to zero, i.e. take only diagrams of type 14 (d) and (e) into account. If, in a later stage, those couplings turn out to be needed (e.g. in order to obtain a quantitative fit to the NN data), they should be included.

There is a further structural difference which has an enormous impact on the results and requires an extended discussion. In general, besides the unitarity cut for $t > (m_{\pi} + m_{\pi})^2$ treated in the dispersion integral (Eq. (8)), there exists a left hand cut for $t < t_0$ in the $NN \rightarrow NN$ amplitude generated by s-channel poles due to nucleon and π -isobar exchange (Fig. 5). t_0 is fixed by the conditions $m_{N\pi}^2 = 0$. There are two solutions for each exchange; the largest value (generated by nucleon exchange) is at $t_0 = 4m_{\pi}^2$, i.e. just below the π threshold. Consequently this branch point will influence the resulting potentials near threshold considerably.

In the π and ρ channels the corresponding potentials act in P-waves and are thus proportional to the on-shell momentum k_0 , with the effect that the corresponding transition potentials start to increase first when approaching the threshold, but are then suppressed by the k_0 factor. In this way one obtains the characteristic structure of a maximum near threshold, which we have observed in such channels. The point now is that both the A_1 and H_1 are

S-waves; therefore the transition potentials do not contain the damping factor k_0 anymore. Indeed, Figs. 18 and 19 show the overwhelming effect of the left hand cut near threshold, in both channels. It essentially remains when correlations (which contain the A_1 resonance) are included, although the influence of the A_1 is clearly seen.

Fig. 20 shows the resulting spectral functions H_P , A_A , and A_P . Again the strong effect of the left hand cut near threshold is obvious. Note also that for H_P , A_1 and H_1 provide roughly similar contributions, but with opposite sign.

In Fig. 21 we present the resulting on-shell potentials in some selected partial waves. For both S-states, the (attractive) A_1 contribution strongly dominates the result arising from the H_1 channel but is considerably smaller (as far as the modulus is concerned) compared to the corresponding piece in the H_P channel, cf. Fig. 17. For 3P_1 both contributions have opposite sign and roughly cancel; the total result is negligible compared to the H_P channel.

In contrast to the H_P , A_A channels discussed before, the above results cannot be suitably parametrized in terms of sharp-mass exchanges. In case of the A_1 , no reasonable mass can be found which works for both spectral functions; moreover all effective coupling constants become strongly t -dependent. The basic reason is again the dominance of the left hand cut, which destroys the conventional bump structure of the spectral functions found in other channels of correlated H_P and A_A exchange.

IV. CONCLUDING REMARKS

In this work we have determined the contribution to the NN interaction due to the exchange of a correlated pair between two nucleons. The correlations between H_P and A_A have been taken into account using a realistic meson exchange model of the H_P interaction [10]. In a first step we evaluated the t -channel amplitude $^H_P \rightarrow ^H_P$ including correlations. The transformation into the s -channel with the help of dispersion-theoretic methods then yields the correlated H_P exchange NN potential. We have investigated four relevant channels of the H_P system characterized by the quantum numbers of the physical particles H_P , A_A , and H_1 .

In the pionic channel correlated H_P exchange yields a short-ranged contribution, which roughly corresponds to an exchange of a heavy (effective) H_P with a mass of about 1 GeV. The additional tensor force generated by this potential is sufficient to compensate for a reduction of the NN cut-off mass m_{NN} from 1.3 GeV to 1.0 GeV in the one-pion-exchange potential. For basic theoretical reasons, such a reduction is highly welcome, since various models of nucleon structure unanimously predict a rather soft NN form factor characterized by $m_{NN} \approx 0.8$ GeV. Such a small value might be reached if correlated H_P exchange is included, too, which is also missing in the Bonn potential. (As usual, stands for a low mass correlated pair in the 0^+ channel.) Thus it appears that in the Bonn potential [2] the one-pion-exchange potential together with a hard form factor is an effective description of 'true' one-pion exchange (with a soft form factor) plus correlated H_P (and A_A) exchange in the pionic channel.

In the H_P channel, the exchange of a correlated pair also provides a sizable contribution to the NN interaction. Since the H_P mass is near the threshold we have included the genuine H_P meson explicitly and replaced the (effective) H_P exchange in the Bonn potential by the resulting correlated H_P potential, which can be decomposed into a pole and a non-pole piece. The former provides a microscopic model for 'true' H_P exchange leading to a renormalized H_P NN coupling constant, $g_{^H_P NN}^2 = 4 = 11.0$, which is about a factor of two smaller than the effective value of 20 used in the Bonn potential. Thus 'true' correlated H_P exchange (Fig. 1 (e)) provides almost half of the empirical repulsion needed in the NN interaction; it can be parametrized by sharp-mass H_P exchange with $g_{^H_P NN}^2 \approx 8.5$, $f_{^H_P NN} = g_{^H_P NN} \approx 0.4$ and $m_{^H_P} \approx 1120$ MeV.

Our present result for the H_P coupling constant ($g_{^H_P NN}^2 = 20g_{^H_P NN}^2$) is well compatible with SU(3), provided that there exists a small, negative NN coupling of vector type, with the magnitude of the order of the H_P -coupling. Such a NN coupling (especially the required negative sign) occurs naturally if it is supposed to arise via the KK continuum. Although corresponding H_P exchange in the NN interaction provides only a small contribution to the repulsion, it makes the above relation between H_P and H_P couplings agree with SU(3) predictions. Consequently there appears to be little room for explicit quark-gluon effects in being responsible for the short-range NN repulsion.

Additional contributions arise in the A_1 and H_1 channels. They are sizable individually, mainly due to left-hand cut effects arising from nucleon and H_P exchange in a S-wave. However, in some partial waves strong cancellations occur between the A_1 and H_1 contributions. Further contributions are, in principle, generated by direct coupling of the A_1/H_1 to the nucleon. The size of such couplings is, however, not known; these terms are therefore omitted in the present work. It remains to be seen whether a precise fit of the NN observables requires such terms and thereby establishes their existence.

In this appendix we derive Eq. (17) of the main text, which provides the connection between the spectral functions needed in Eq. (8) and the imaginary part of the $N\bar{N} \rightarrow N\bar{N}$ amplitude in the LSJ basis (${}^J N$) obtained from the unitarity relation (Eq. (9)). For the latter it was necessary to work in the LSJ basis in order to identify the allowed $N\bar{N} \rightarrow N\bar{N}$ transitions. In order to establish the connection to the spectral functions however, matrix elements of the invariants \hat{C}_j are required, which is most suitably done in the helicity state basis. The imaginary part of the $N\bar{N} \rightarrow N\bar{N}$ amplitude is now defined by (cf. Eq. (12) for the analogous definition in LSJ basis) ${}^J N \left(\begin{smallmatrix} 0 & 0 \\ N & N \end{smallmatrix}; \begin{smallmatrix} 0 & 0 \\ N & N \end{smallmatrix} \right)$ $\text{Im } T^J \left(\begin{smallmatrix} 0 & 0 & 0 \\ N & N & N \end{smallmatrix}; \begin{smallmatrix} 0 & 0 \\ N & N \end{smallmatrix}; \bar{t} \right)$ and the relation between LSJ and helicity basis amplitudes is given by the standard expressions (cf. [2])

$$\begin{aligned}
 {}^J N_1 &= \frac{1}{2} {}^J N (J0;J0) + a^2 {}^J N (J-11;J-11) - ab {}^J N (J+11;J-11) \\
 &\quad - ab {}^J N (J-11;J+11) + b^2 {}^J N (J+11;J+11) \\
 {}^J N_2 &= \frac{1}{2} {}^J N (J0;J0) + a^2 {}^J N (J-11;J-11) - ab {}^J N (J+11;J-11) \\
 &\quad - ab {}^J N (J-11;J+11) + b^2 {}^J N (J+11;J+11) \\
 {}^J N_3 &= \frac{1}{2} {}^J N (J1;J1) + b^2 {}^J N (J-11;J-11) + ab {}^J N (J+11;J-11) \\
 &\quad + ab {}^J N (J-11;J+11) + a^2 {}^J N (J+11;J+11) \\
 {}^J N_4 &= \frac{1}{2} {}^J N (J1;J1) + b^2 {}^J N (J-11;J-11) + ab {}^J N (J+11;J-11) \\
 &\quad + ab {}^J N (J-11;J+11) + a^2 {}^J N (J+11;J+11) \\
 {}^J N_5 &= -ab {}^J N (J-11;J-11) - b^2 {}^J N (J+11;J-11) + a^2 {}^J N (J-11;J+11) \\
 &\quad - ab {}^J N (J+11;J+11) \\
 {}^J N_6 &= {}^J N_5 \quad (\text{on shell})
 \end{aligned} \tag{A1}$$

where we used the short-hand notation for the ${}^J N$ amplitudes defined in Table V and

$$a = \frac{s}{2(2J+1)} \quad b = \frac{s}{2(2J+1)} : \tag{A2}$$

The various channel contributions to $\text{Im } T \left(\begin{smallmatrix} 0 & 0 & 0 \\ N & N & N \end{smallmatrix}; \begin{smallmatrix} 0 & 0 \\ N & N \end{smallmatrix}; \bar{t} \right)$ are then given by

$$\begin{aligned}
 :N_i &= N \left(\begin{smallmatrix} 0 & 0 \\ N & N \end{smallmatrix}; \begin{smallmatrix} 0 & 0 \\ N & N \end{smallmatrix} \right) \frac{1}{4} d^0_{00}(\cos\#) {}^0 N \left(\begin{smallmatrix} 0 & 0 \\ N & N \end{smallmatrix}; \begin{smallmatrix} 0 & 0 \\ N & N \end{smallmatrix} \right) \frac{1}{4} d^0_{00}(\cos\#) {}^0 N_i \\
 ;!;A_1;H_1 :N_i &= N \left(\begin{smallmatrix} 0 & 0 \\ N & N \end{smallmatrix}; \begin{smallmatrix} 0 & 0 \\ N & N \end{smallmatrix} \right) \frac{3}{4} d^1_{00}(\cos\#) {}^1 N \left(\begin{smallmatrix} 0 & 0 \\ N & N \end{smallmatrix}; \begin{smallmatrix} 0 & 0 \\ N & N \end{smallmatrix} \right) \frac{3}{4} d^1_{00}(\cos\#) {}^1 N_i
 \end{aligned} \tag{A3}$$

We now define a vector $N = (N_1, N_2, N_3, N_4, N_5, N_6)^T$, $!;A_1;H_1$, and use Eqs. (15) and (A1) to express its components in terms of the LSJ amplitudes ${}^J N (L^0 S^0; LS)$ for each of the contributing channels. We obtain

$$N = \begin{pmatrix} 0 \\ \frac{1}{8} {}^0 N (00;00) \\ \frac{1}{8} {}^0 N (00;00) \\ 0 \\ 0 \\ 0 \end{pmatrix} \begin{matrix} 1 \\ C \\ C \\ C \\ A \\ A \end{matrix} ; \tag{A4}$$

$$N^{A_1} = \begin{pmatrix} 0 \\ 0 \\ \frac{3(1+\cos\#)}{16} {}^1 N (11;11) \\ \frac{3(1+\cos\#)}{16} {}^1 N (11;11) \\ 0 \end{pmatrix} \begin{matrix} 1 \\ C \\ C \\ C \\ A \end{matrix} ; \tag{A5}$$

$$N^{H_1} = \begin{matrix} 0 & \frac{3 \cos \#}{8} {}^1 N(00;00) & 1 \\ \frac{3 \cos \#}{8} {}^1 N(00;00) & 0 & C \\ 0 & 0 & C \\ 0 & 0 & A \end{matrix}; \quad (A 6)$$

$$N^! = \begin{matrix} 0 & \frac{3}{4} \cos \# [\frac{1}{6} {}^1 N(01;01) & \frac{2}{9} {}^1 N(01;21) + \frac{1}{3} {}^1 N(21;21)] & 1 \\ \frac{3}{4} \cos \# [\frac{1}{6} {}^1 N(01;01) & \frac{2}{9} {}^1 N(01;21) + \frac{1}{3} {}^1 N(21;21)] & C \\ \frac{1}{16} (1 + \cos \#) [2 {}^1 N(01;01) + 2 \sqrt{2} {}^1 N(01;21) + {}^1 N(21;21)] & C \\ \frac{1}{16} (1 + \cos \#) [2 {}^1 N(01;01) + 2 \sqrt{2} {}^1 N(01;21) + {}^1 N(21;21)] & C \\ \frac{1}{16} \sin \# [2 {}^1 N(01;01) + 2 \sqrt{2} {}^1 N(01;21) + {}^1 N(21;21)] & A \end{matrix} : \quad (A 7)$$

The decomposition of the imaginary part of Eq. (4) can now be written for the helicity state matrix-elements in matrix notation

$$N^! ; A_1 ; H_1 = \begin{matrix} 0 & S_1 & V_1 & T_1 & P_1 & A_1 & 1 \\ S_2 & V_2 & T_2 & P_2 & A_2 & C \\ S_3 & V_3 & T_3 & P_3 & A_3 & C \\ S_4 & V_4 & T_4 & P_4 & A_4 & A \\ S_5 & V_5 & T_5 & P_5 & A_5 & R \end{matrix} M R \quad (A 8)$$

where $R = (S \ V \ T \ P \ A)$. S_i, V_i, T_i, P_i , and A_i are helicity state matrix-elements of the Fermi invariants using the same indexing as for the N amplitudes and we find

$$M = \begin{matrix} 0 & 2 & 1 & \cos \# & 2 \cos \# & 2 & 1 & 1 \\ 2 & 1 & \cos \# & 2 \cos \# (2^2 + 1) & 2 & 1 & C \\ 0 & 2(1 + \cos \#) & 2(1 + \cos \#) & 0 & (2^2 - 1)(1 + \cos \#) & C \\ 0 & 2(1 - \cos \#) & 2(1 - \cos \#) & 0 & (2^2 - 1)(1 - \cos \#) & A \\ 0 & \sin \# & 2 \sin \# & 0 & 0 & \end{matrix} \quad (A 9)$$

The spectral functions are then simply obtained by calculating $R = M^{-1} N^! ; A_1 ; H_1$ yielding the result of Eq. (17).

[1] G. Janssen, B.C. Pearce, K. Holinde, and J. Speth, Phys. Rev. D (in print).
[2] R. Machleidt, K. Holinde, and Ch. Elster, Phys. Rep. 149, 1 (1987).
[3] G. Janssen, K. Holinde, and J. Speth, Phys. Rev. Lett. 73, 1332 (1994).
[4] T.E.O. Ericson and M. Rosa-Clot, Nucl. Phys. A 405, 497 (1983).
[5] T.E.O. Ericson and M. Rosa-Clot, Ann. Rev. Nucl. Part. Sci. 35, 271 (1985).
[6] K.F. Liu, S.J. Dong, T. Dapper, and W. Wilcox, Phys. Rev. Lett. 74, 2172 (1995).
[7] S.A. Coon and M.D. Scadron, Phys. Rev. C 23, 1150 (1981).
[8] S.A. Coon and M.D. Scadron, Phys. Rev. D 42, 2256 (1990).
[9] A.W. Thomas and K. Holinde, Phys. Rev. Lett. 63, 2025 (1989).
[10] G. Janssen, K. Holinde, and J. Speth, Phys. Rev. C 49, 2763 (1994).
[11] H.-C. Kim, J.W. Durso, and K. Holinde, Phys. Rev. C 49, 2355 (1994).
[12] R. Blankenbecler and R. Sugar, Phys. Rev. 142, 1051 (1966).
[13] V. Mull, J. Haidenbauer, T. Hippchen, and K. Holinde, Phys. Rev. C 44, 1337 (1991).
[14] R. Aaron, Modern Three-Hadron Physics (Springer Verlag, Heidelberg, 1976).
[15] A.D. Martin and T.D. Spearman, Elementary Particle Theory (North-Holland, Amsterdam, 1970).
[16] C. Schutz, J.W. Durso, K. Holinde, and J. Speth, Phys. Rev. C 49, 2671 (1994).
[17] K. Holinde and A.W. Thomas, Phys. Rev. C 42, R1195 (1990).
[18] J. Haidenbauer, K. Holinde, and A.W. Thomas, Phys. Rev. C 49, 2331 (1994).
[19] T. Ueda, Phys. Rev. Lett. 68, 142 (1992).
[20] G. Hoehler and E. Pietarinen, Nucl. Phys. B 95, 210 (1975).
[21] V. Mull, private communication.

[22] J. A. Dankowych et al., Phys. Rev. Lett. 38, 580 (1981).

FIG. 1. Contributions to the NN potential. (a) is generated by the scattering equation whereas (b) and (c) are explicitly contained in the Bonn potential. (d) shows correlated exchange treated in the present work.

FIG. 2. Diagram visualizing the NN scattering process, in the s (NN → NN) and t (N \bar{N} → N \bar{N}) channels.

FIG. 3. Diagram visualizing the exchange contribution to the NN interaction.

FIG. 4. The transition amplitude $t_{N\bar{N}}$.

FIG. 5. The transition potential $v_{N\bar{N}}$.

FIG. 6. Contributions to the potential.

FIG. 7. Results of our interaction model for the mass distribution in the H₁ and A₁ channels compared with experiment [22].

FIG. 8. The (imaginary) transition potential $v_{N\bar{N}}$ (dashed curve) in the pion channel together with the corresponding amplitude $t_{N\bar{N}}$. The dotted line shows the real part of t , the solid line the imaginary part.

FIG. 9. The spectral function in the pionic channel $\rho(t)$. The dotted line shows the uncorrelated part whereas the solid line represents the correlated contribution.

FIG. 10. On-shell NN potential V_{NN} as function of the nucleon lab energy in the 1S_0 state (a) and $^3D_1 \rightarrow ^3S_1$ transition (b). The dotted line denotes the one-pion-exchange potential as used in the Bonn potential ($g_{NN}^2 = 4 = 14.4$; $m_{NN} = 1.3$ GeV). For the dashed line, $m_{NN} = 1.0$ GeV. The solid line results if correlated exchange in the pionic channel is added to the dashed line.

FIG. 11. Diagrams contributing to the NN form factor.

FIG. 12. The t-dependent effective NN coupling constant for various values of m_0 .

FIG. 13. The (imaginary) transition potential $v_{N\bar{N}}$ (dashed curve) in the π channel (a) together with the corresponding amplitude $t_{N\bar{N}}$ (b). The dotted line shows the real part of t , the solid line the imaginary part.

FIG. 14. Contributions to the NN potential in the π channel.

FIG. 15. The spectral functions in the π channel. As explained in the text the dashed line contains only the ρ -function contribution of diagrams 14 (a)-(d) whereas the dash-dotted line shows the vertex and propagator corrections to the corresponding diagrams. The dotted line contains only the non-pole part (14 (e)) and the solid line shows the full result.

FIG. 16. On-shell NN potential V_{NN} as function of the nucleon lab energy in the 1S_0 and 3P_1 state. The long-dashed line shows the result of single π exchange as contained in the Bonn potential ($g_{\pi NN}^2 = 4 = 20$; $m_\pi = 1500$ MeV). The dashed line contains only the π -function contribution of the diagrams of Figs. 14 (a)–(d) (cf. text) from which the dash-dotted line is obtained by adding the vertex and propagator corrections contained in the corresponding diagrams. The full result is shown by the solid line and contains in addition the non-pole part (Fig. 14 (e)).

FIG. 17. The t -dependent effective π NN vector coupling constant $g_{\pi NN}^2 = 4$ and the ratio $f_{\pi NN} = g_{\pi NN} / m_\pi$ for $m_\pi = 1120$ MeV (solid). The dashed line shows $g_{\pi NN}^2 = 4$ when the physical π mass (782.6 MeV) is used.

FIG. 18. The (real) transition potential v_{NN}^- (dashed curve) in the A_1 channel together with the corresponding amplitude t_{NN}^- . The dotted line shows the real part of t , the solid line the imaginary part.

FIG. 19. Same as Fig. 18 but for the H_1 channel.

FIG. 20. The spectral functions in the A_1 and H_1 channel (a): H_1 ; (b): A_1 ; (c): A_1 . The dashed line shows the contribution of the pole part whereas the dotted line contains the non-pole part. The full result is given by the solid line.

FIG. 21. On-shell NN potential V_{NN} as function of the nucleon lab energy in the 1S_0 , 3S_1 , and 3P_1 states. The dash-dotted (dotted) line shows correlated π exchange in the A_1 (H_1) channel.

TABLE I. Quantum numbers and possible transitions from the NN^- to the NN^- system.

	J^P	(I^G)	L	S	L_{NN^-}	S_{NN^-}	$L_{NN^-} S_{NN^-} !$	L S	notation
π	0	(1 ⁻)	1	1	0	0	J 0 ! J+ 1 1		t_{π}^+
ρ	1	(0 ⁻)	1	1	0	1	J 1 1 ! J 1		t_{ρ}^-
A_1	1 ⁺	(1 ⁻)	0	1	1	1	J+ 1 1 ! J 1		$t_{A_1}^-$
A_1	1 ⁺	(1 ⁻)	2	1	1	1	J 1 ! J+ 1 1		$t_{A_1}^+$
H_1	1 ⁺	(0 ⁻)	0	1	1	0	J 0 ! J 1 1		$t_{H_1}^-$
H_1	1 ⁺	(0 ⁻)	2	1	1	0	J 0 ! J+ 1 1		$t_{H_1}^+$

TABLE II. Isospin factors for the $NN^- \pi$ transition potential.

Exchange particle	Type of diagram	$I=0$	$I=1$
N	s	$\frac{p}{6}$	-2
ρ	s	$-\frac{p}{6}$	$\frac{2}{3}$
π	t	$-\frac{p}{6}$	0

TABLE III. Coupling constants and cutoff masses for the $NN\bar{N}$ transition potential.

Vertex	$g^2=4$		[MeV]
NN	14.4	-	1970
NN	0.84	6.1	1970
N	0.36	-	1150
N	20.45	-	1150
NN!	19.42	-	1414

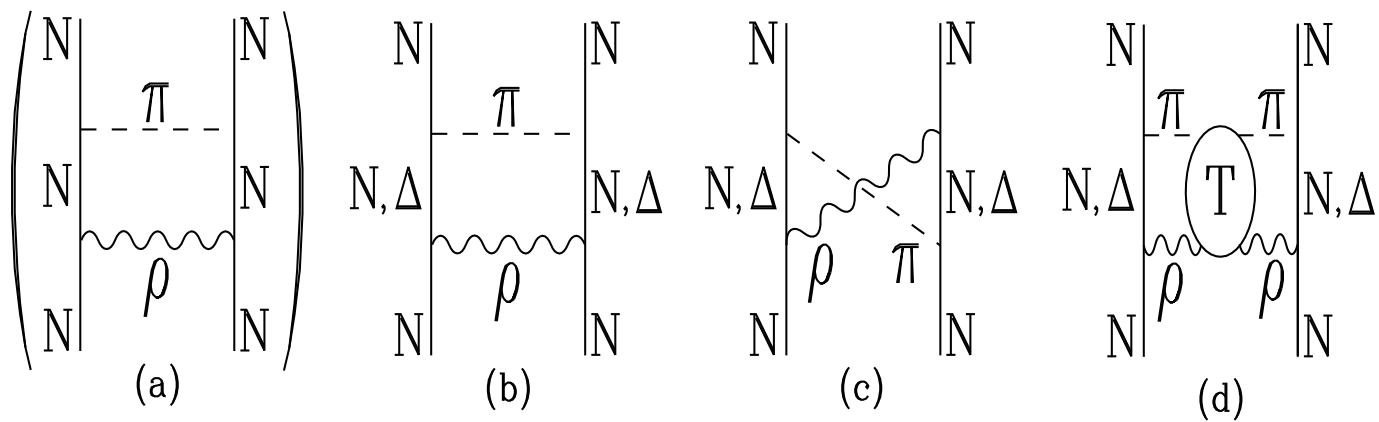
 TABLE IV. Deuteron properties predicted by the model including a soft NN form factor ($\Lambda_{NN} = 1\text{GeV}$) and correlated exchange in comparison to the full Bonn potential and experiment.

	present model	full Bonn potential	experimental data ^a
Binding energy E_d [MeV]	2.2246	2.2247	2.2245754
D state probability P_d [%]	4.37	4.25	-
Quadrupole moment Q_d [fm^2]	0.2781	0.2807	0.2859 0.0003
Asymptotic D/S ratio	0.0265	0.0267	0.0271 0.0008

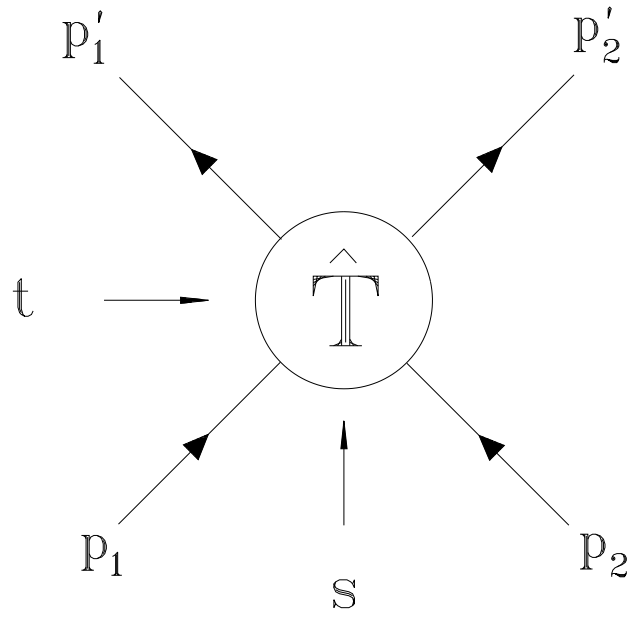
^aReferences are given in [2].

TABLE V. NN matrix elements in helicity basis.

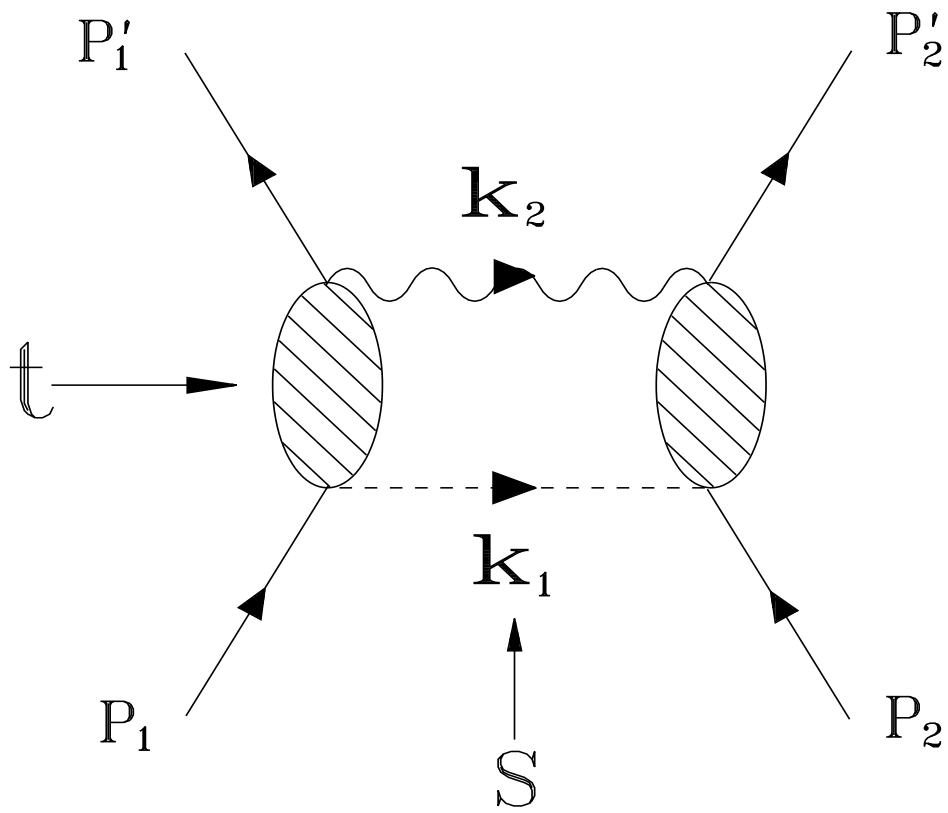
$\langle \begin{smallmatrix} 0 \\ N \end{smallmatrix} \begin{smallmatrix} 0 \\ N \end{smallmatrix} \begin{smallmatrix} J \\ N \end{smallmatrix} \begin{smallmatrix} j \\ N \end{smallmatrix} \begin{smallmatrix} \bar{N} \\ N \end{smallmatrix} \rangle \left(= \frac{1}{2} \right)$
$\begin{smallmatrix} J \\ N \end{smallmatrix} \begin{smallmatrix} + \\ + \end{smallmatrix} \begin{smallmatrix} j \\ N \end{smallmatrix} \begin{smallmatrix} + \\ + \end{smallmatrix} \begin{smallmatrix} + \\ + \end{smallmatrix} \begin{smallmatrix} + \\ + \end{smallmatrix} \rangle$
$\begin{smallmatrix} J \\ N \end{smallmatrix} \begin{smallmatrix} + \\ + \end{smallmatrix} \begin{smallmatrix} j \\ N \end{smallmatrix} \begin{smallmatrix} j \\ + \end{smallmatrix} \begin{smallmatrix} + \\ + \end{smallmatrix} \begin{smallmatrix} + \\ + \end{smallmatrix} \rangle$
$\begin{smallmatrix} J \\ N \end{smallmatrix} \begin{smallmatrix} + \\ + \end{smallmatrix} \begin{smallmatrix} j \\ N \end{smallmatrix} \begin{smallmatrix} j \\ + \end{smallmatrix} \begin{smallmatrix} + \\ + \end{smallmatrix} \begin{smallmatrix} + \\ + \end{smallmatrix} \rangle$
$\begin{smallmatrix} J \\ N \end{smallmatrix} \begin{smallmatrix} + \\ + \end{smallmatrix} \begin{smallmatrix} j \\ N \end{smallmatrix} \begin{smallmatrix} j \\ + \end{smallmatrix} \begin{smallmatrix} + \\ + \end{smallmatrix} \begin{smallmatrix} + \\ + \end{smallmatrix} \rangle$
$\begin{smallmatrix} J \\ N \end{smallmatrix} \begin{smallmatrix} + \\ + \end{smallmatrix} \begin{smallmatrix} j \\ N \end{smallmatrix} \begin{smallmatrix} j \\ + \end{smallmatrix} \begin{smallmatrix} + \\ + \end{smallmatrix} \begin{smallmatrix} + \\ + \end{smallmatrix} \rangle$
$\begin{smallmatrix} J \\ N \end{smallmatrix} \begin{smallmatrix} + \\ + \end{smallmatrix} \begin{smallmatrix} j \\ N \end{smallmatrix} \begin{smallmatrix} j \\ + \end{smallmatrix} \begin{smallmatrix} + \\ + \end{smallmatrix} \begin{smallmatrix} + \\ + \end{smallmatrix} \rangle$



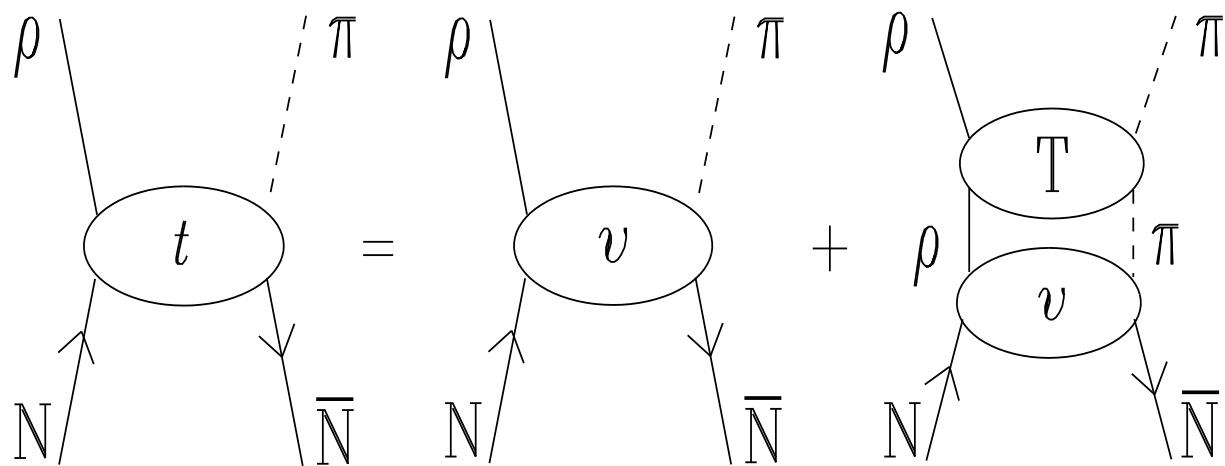
G. Janssen, K. Holinde, and J. Speth
 Correlated ...
 Fig. 1



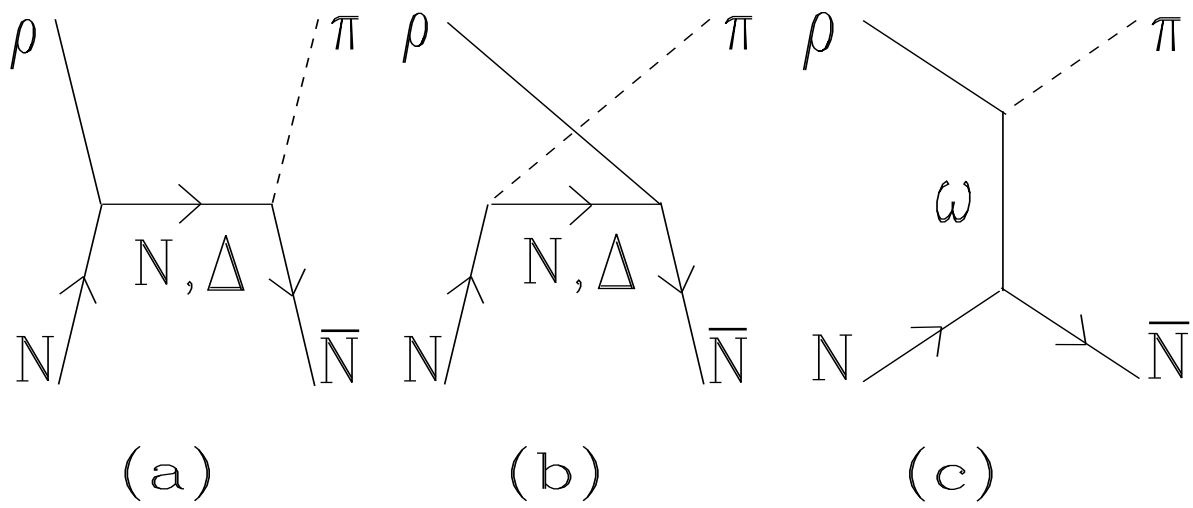
G. Janssen, K. Holinde, and J. Speth
Correlated ...
Fig. 2



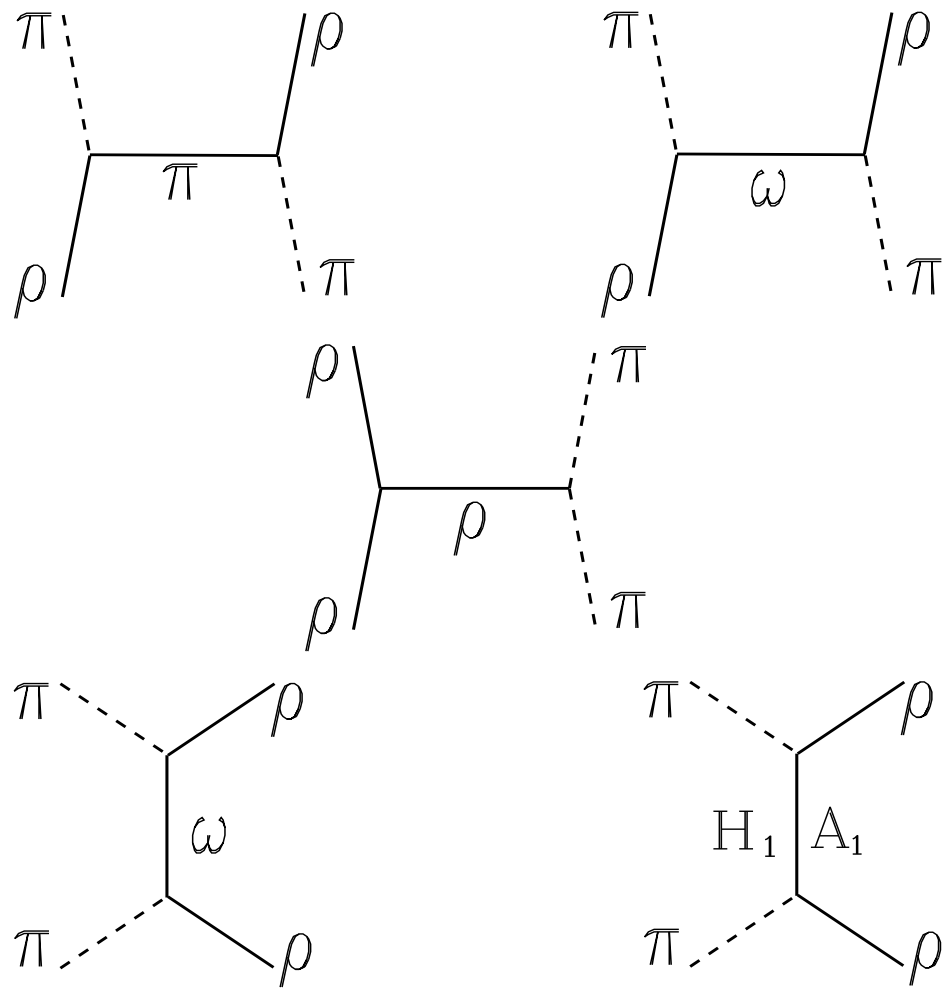
G. Janssen, K. Holinde, and J. Speth
Correlated ...
Fig. 3



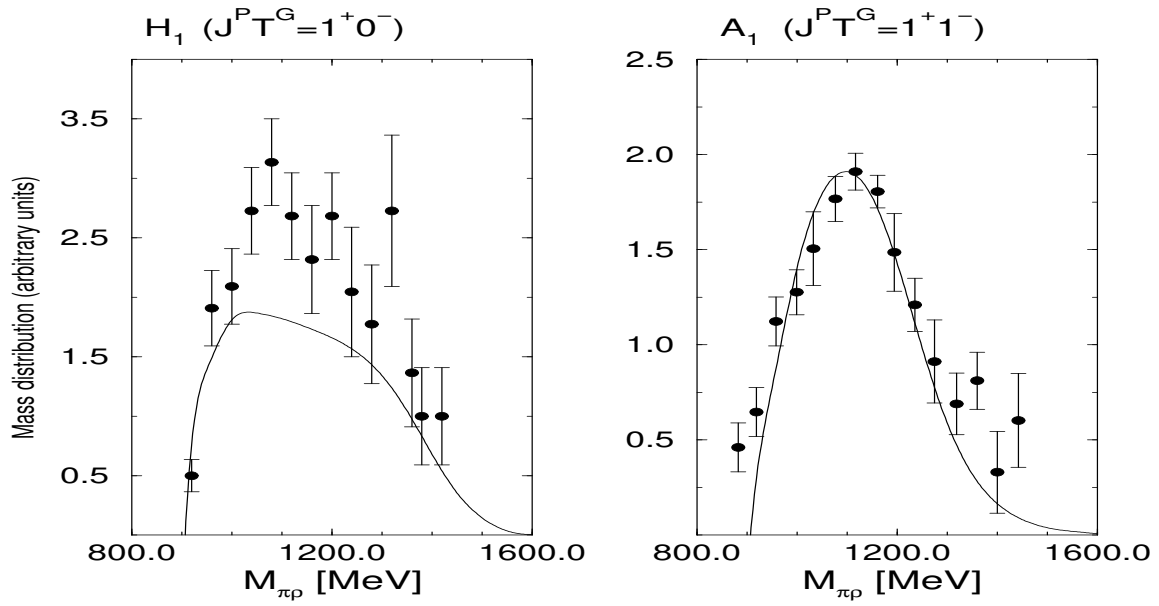
G. Janssen, K. Holinde, and J. Speth
 Correlated ...
 Fig. 4



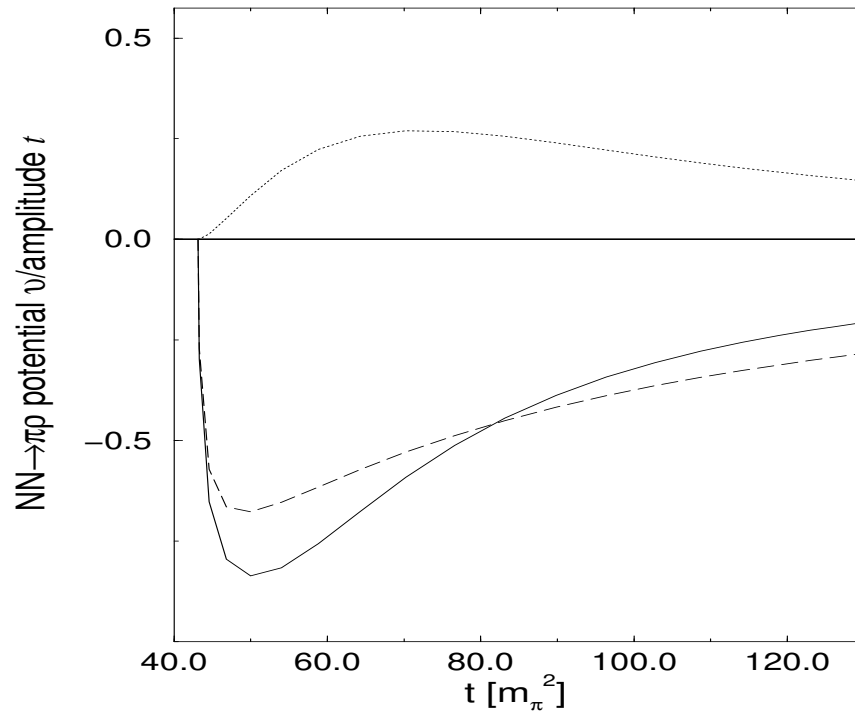
G. Janssen, K. Holinde, and J. Speth
 Correlated ...
 Fig. 5



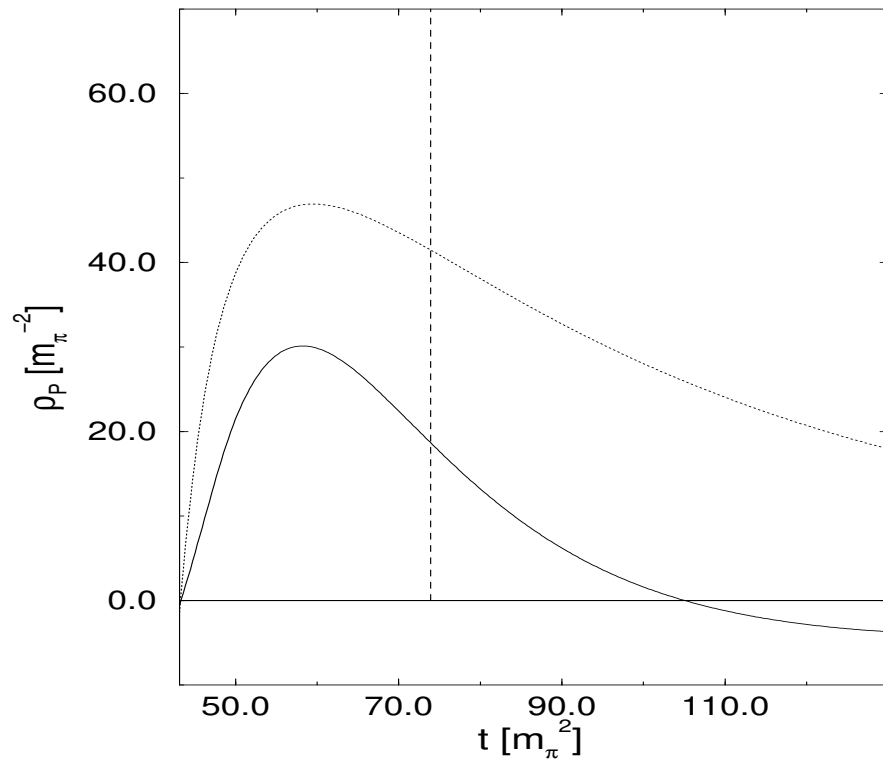
G. Janssen, K. Holinde, and J. Speth
 Correlated ...
 Fig. 6



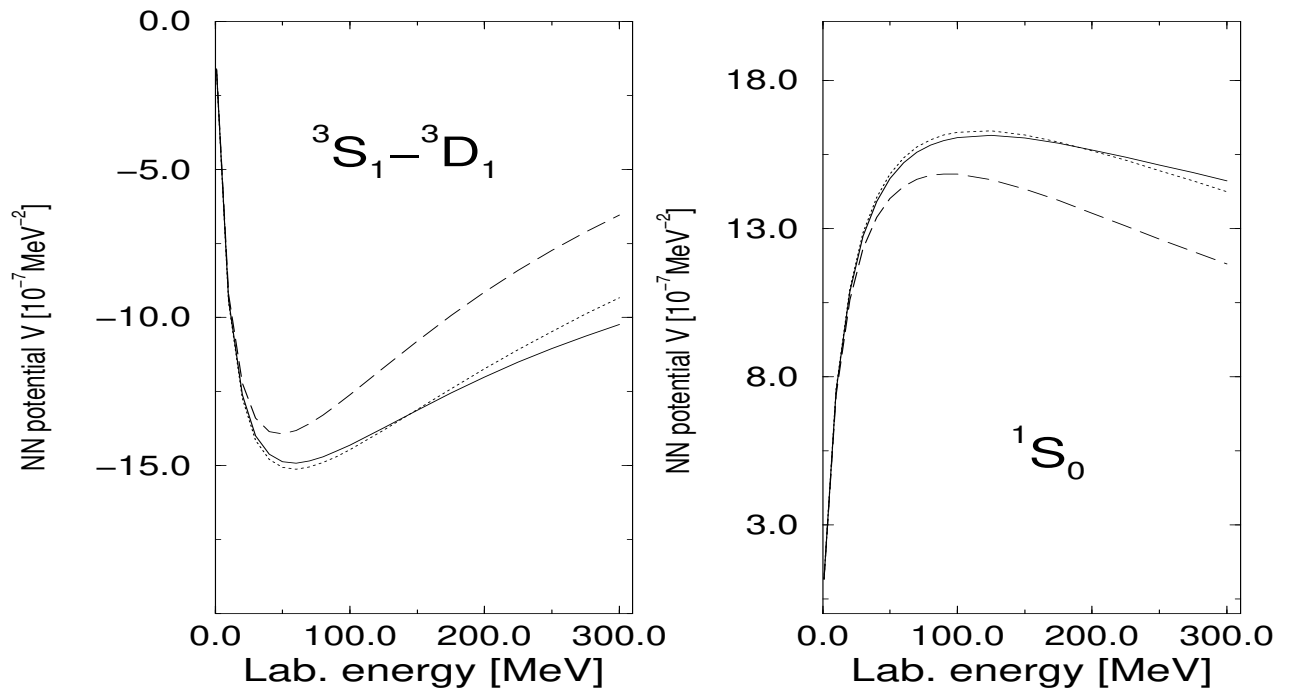
G. Janssen, K. Holinde, and J. Speth
Correlated ...
Fig. 7



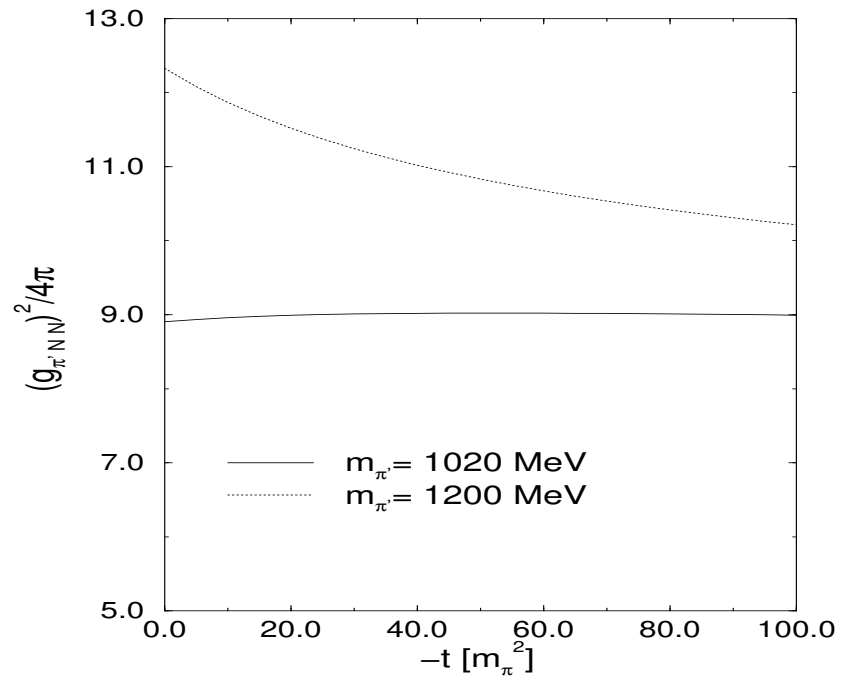
G. Janssen, K. Holinde, and J. Speth
Correlated ...
Fig. 8



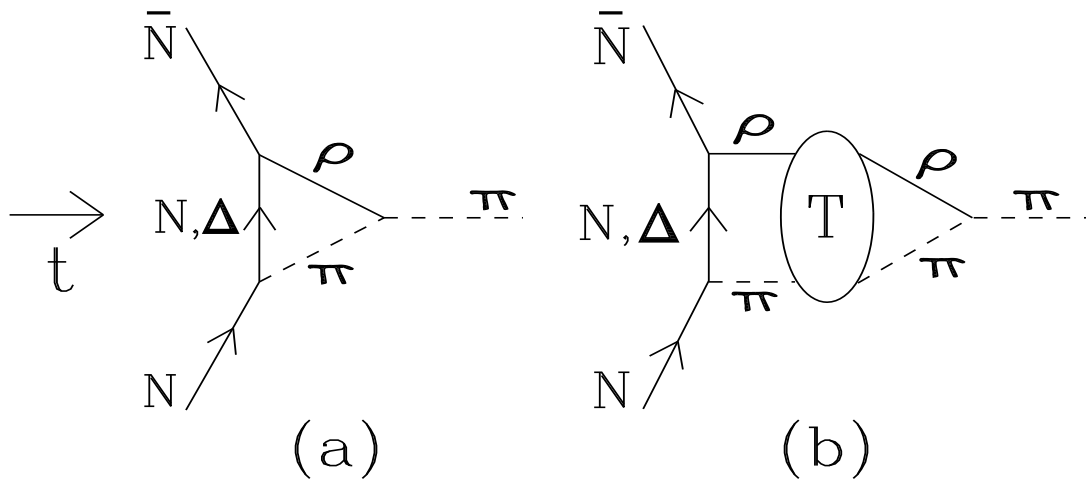
G. Janssen, K. Holinde, and J. Speth
Correlated ...
Fig. 9



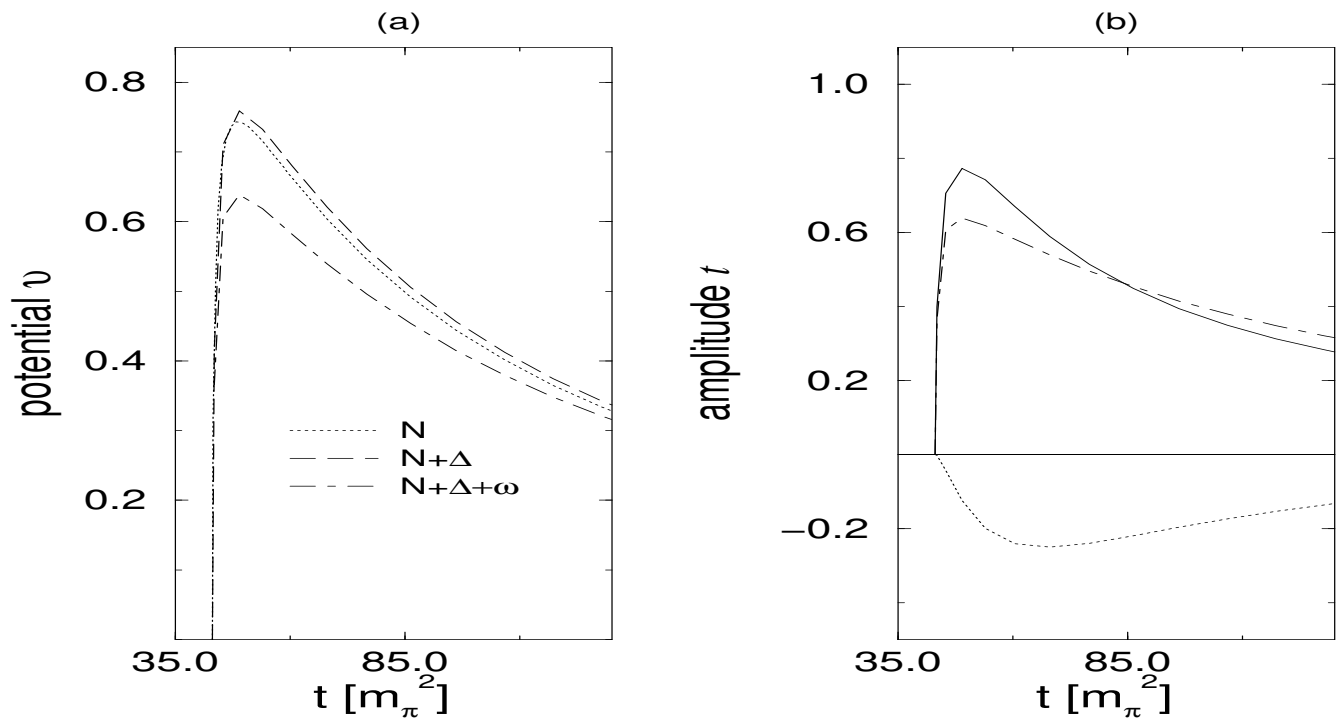
G. Janssen, K. Holinde, and J. Speth
Correlated ...
Fig. 10



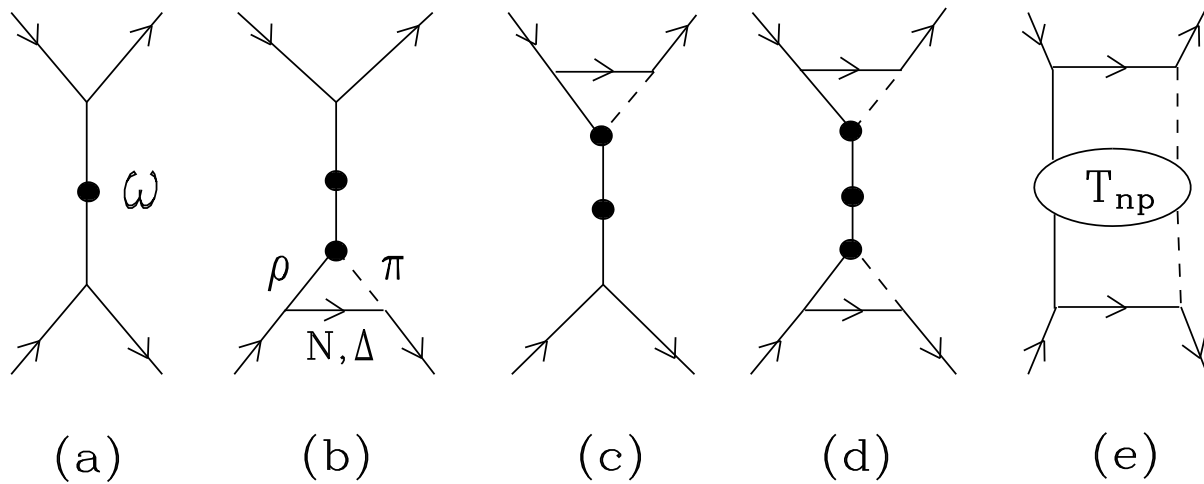
G. Janssen, K. Holinde, and J. Speth
Correlated ...
Fig. 11



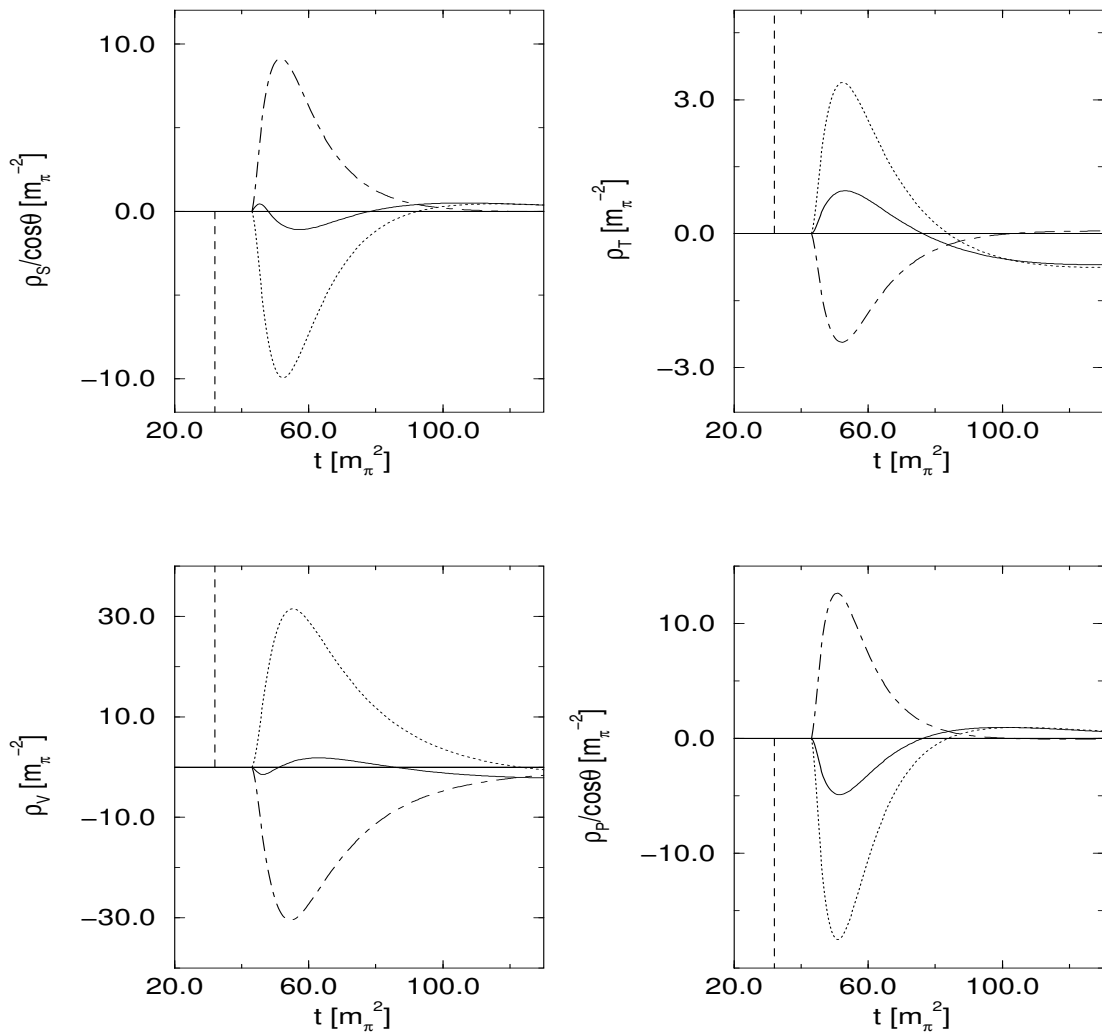
G. Janssen, K. Holinde, and J. Speth
 Correlated ...
 Fig. 12



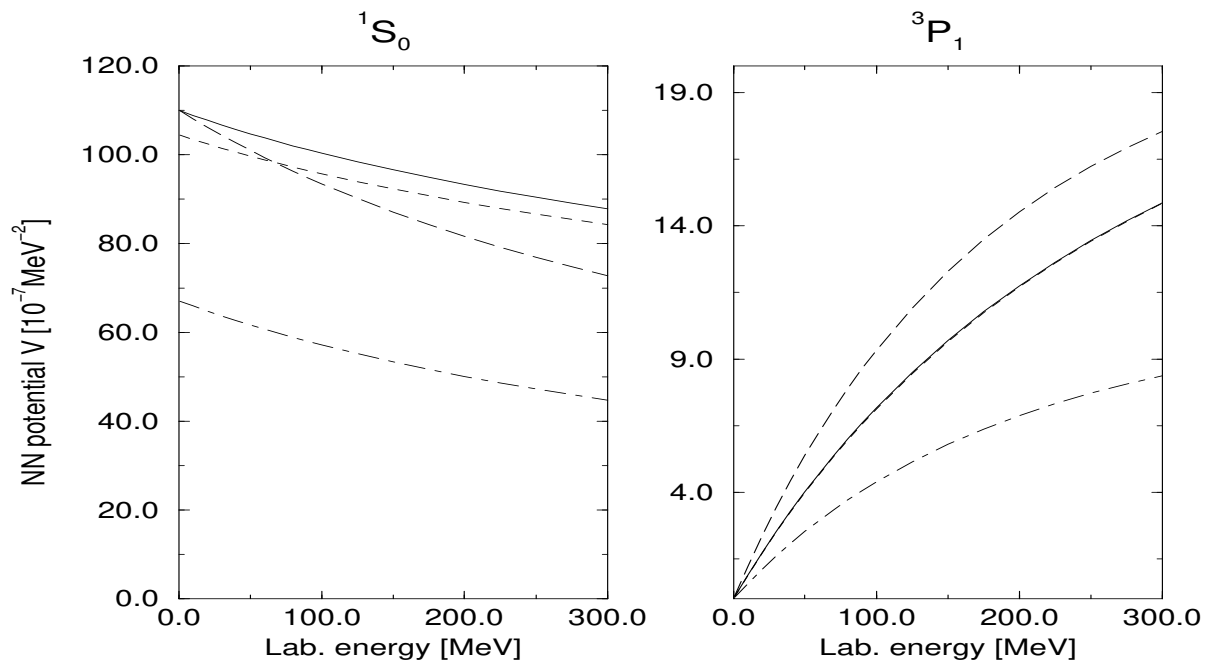
G. Janssen, K. Holinde, and J. Speth
 Correlated ...
 Fig. 13



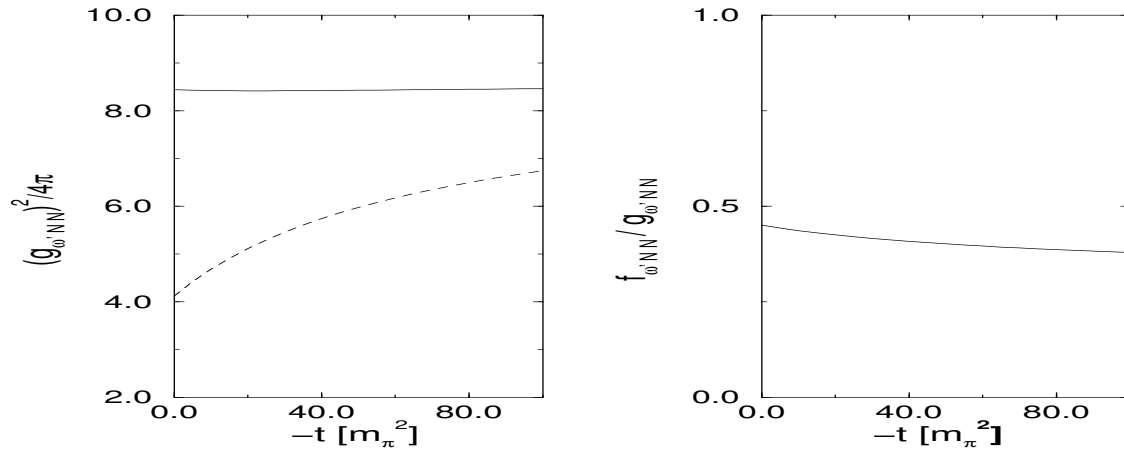
G. Janssen, K. Holinde, and J. Speth
 Correlated ...
 Fig. 14



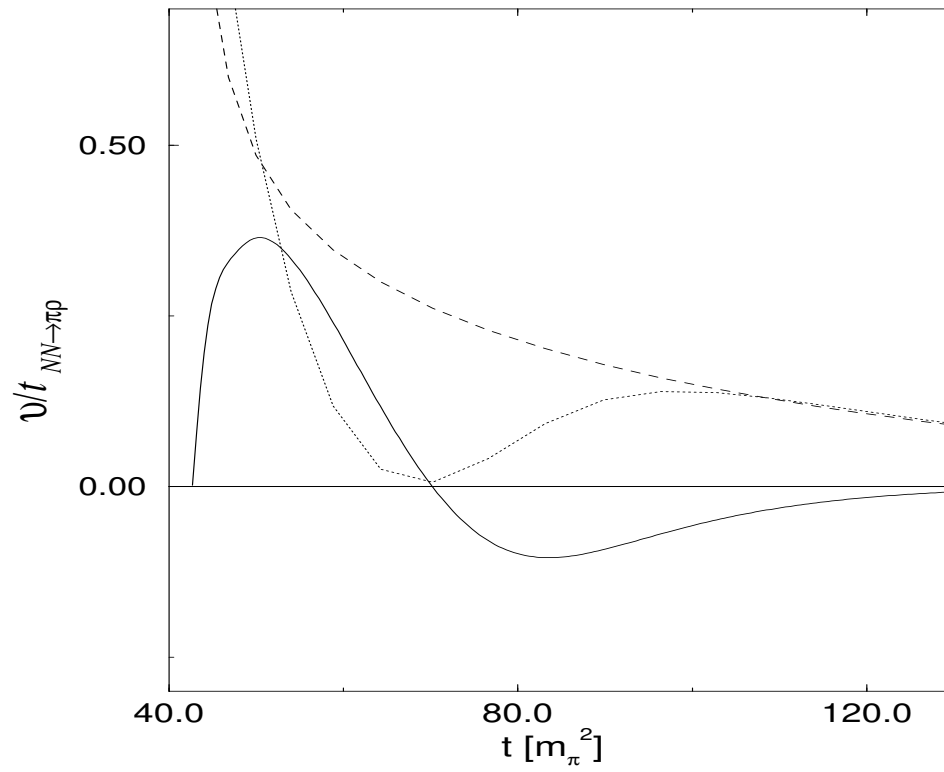
G. Janssen, K. Holinde, and J. Speth
 Correlated ...
 Fig. 15



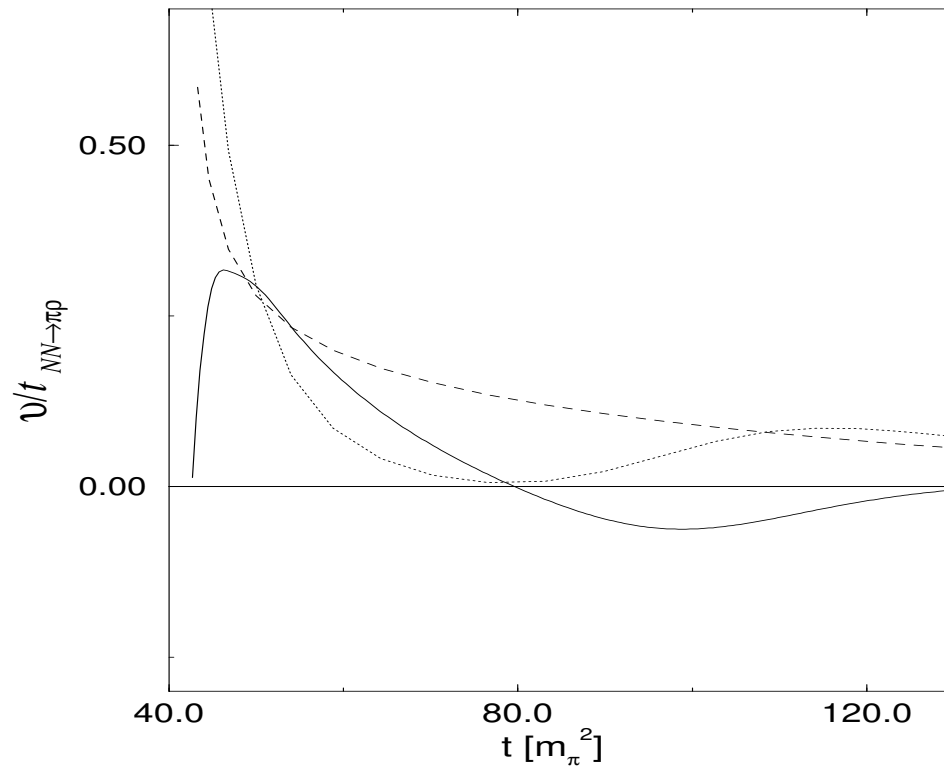
G. Janssen, K. Holinde, and J. Speth
Correlated ...
Fig. 16



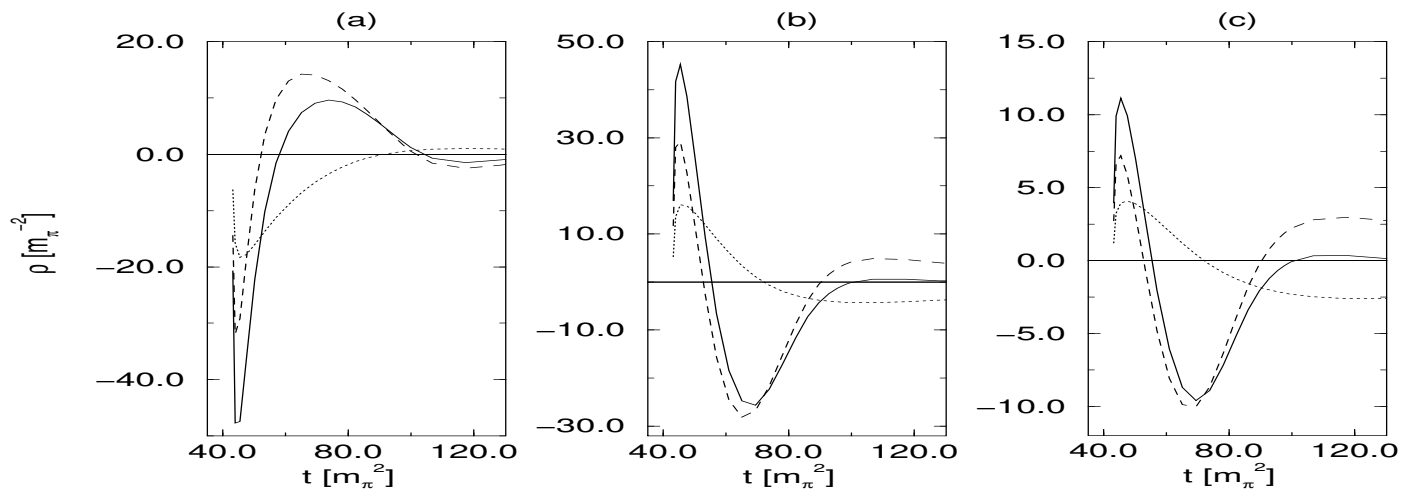
G. Janssen, K. Holinde, and J. Speth
Correlated ...
Fig. 17



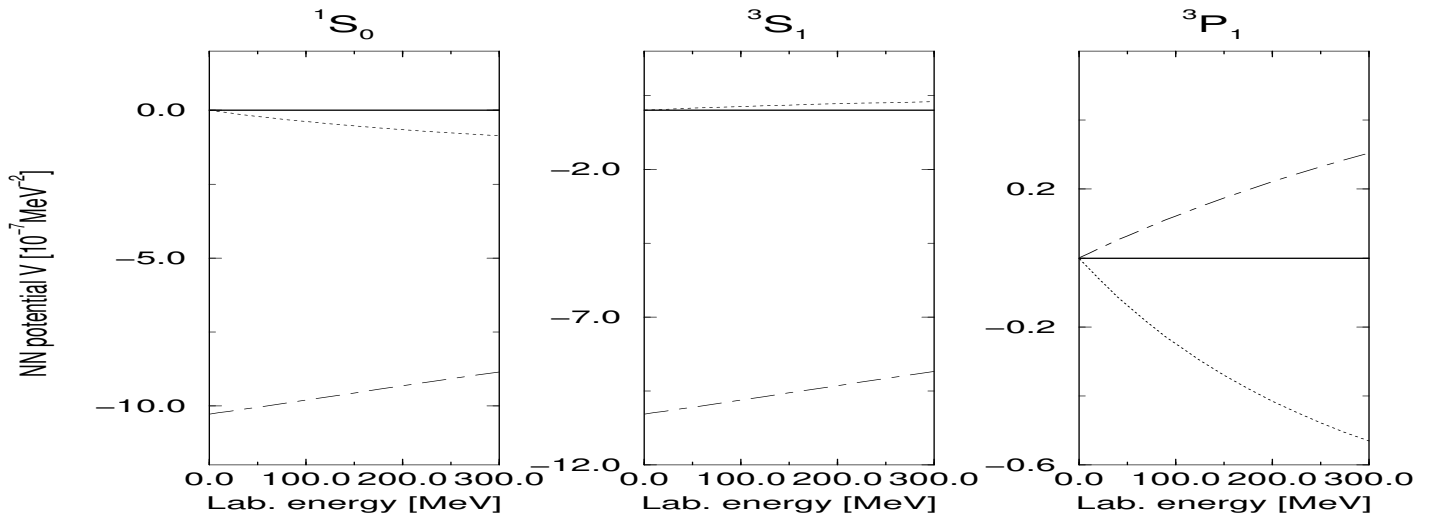
G. Janssen, K. Holinde, and J. Speth
Correlated ...
Fig. 18



G. Janssen, K. Holinde, and J. Speth
Correlated ...
Fig. 19



G. Janssen, K. Holinde, and J. Speth
Correlated ...
Fig. 20



G. Janssen, K. Holinde, and J. Speth
 Correlated ...
 Fig. 21